

Review

Propylene Synthesis: Recent Advances in the Use of Pt-Based Catalysts for Propane Dehydrogenation Reaction

Marco Martino ^{*}, Eugenio Meloni , Giovanni Festa and Vincenzo Palma 

Department of Industrial Engineering, University of Salerno, Via Giovanni Paolo II 132, 84084 Fisciano, SA, Italy; emeloni@unisa.it (E.M.); gifesta@unisa.it (G.F.); vpalma@unisa.it (V.P.)

* Correspondence: mamartino@unisa.it; Tel.: +39-089-964027

Abstract: Propylene is one of the most important feedstocks in the chemical industry, as it is used in the production of widely diffused materials such as polypropylene. Conventionally, propylene is obtained by cracking petroleum-derived naphtha and is a by-product of ethylene production. To ensure adequate propylene production, an alternative is needed, and propane dehydrogenation is considered the most interesting process. In literature, the catalysts that have shown the best performance in the dehydrogenation reaction are Cr-based and Pt-based. Chromium has the non-negligible disadvantage of toxicity; on the other hand, platinum shows several advantages, such as a higher reaction rate and stability. This review article summarizes the latest published results on the use of platinum-based catalysts for the propane dehydrogenation reaction. The manuscript is based on relevant articles from the past three years and mainly focuses on how both promoters and supports may affect the catalytic activity. The published results clearly show the crucial importance of the choice of the support, as not only the use of promoters but also the use of supports with tuned acid/base properties and particular shape can suppress the formation of coke and prevent the deep dehydrogenation of propylene.

Keywords: propane dehydrogenation; propylene; platinum; catalysis



Citation: Martino, M.; Meloni, E.; Festa, G.; Palma, V. Propylene Synthesis: Recent Advances in the Use of Pt-Based Catalysts for Propane Dehydrogenation Reaction. *Catalysts* **2021**, *11*, 1070. <https://doi.org/10.3390/catal11091070>

Academic Editors:
Stanislaw Waclawek, Dionysios (Dion) D. Dionysiou,
Andrzej Kudelski and Jochen A. Lauterbach

Received: 10 August 2021
Accepted: 2 September 2021
Published: 3 September 2021

Publisher's Note: MDPI stays neutral with regard to jurisdictional claims in published maps and institutional affiliations.



Copyright: © 2021 by the authors. Licensee MDPI, Basel, Switzerland. This article is an open access article distributed under the terms and conditions of the Creative Commons Attribution (CC BY) license (<https://creativecommons.org/licenses/by/4.0/>).

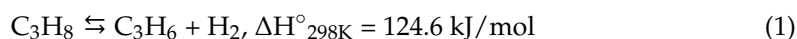
1. Introduction

Propylene [1] is the feedstock of strategic materials such as acrolein, polypropylene, acetone, polyacrylonitrile, propylene oxide and other industrial products [2]. The conventional propylene production industrial processes are the fluid catalytic cracking and the naphtha and light diesel steam cracking [3]. The fast consumption of fossil fuels is making conventional propylene production methods unsuitable to meet the growing demand for propylene; therefore, the development of more efficient and economical production methods is a major concern [4]. Innovative methods to produce propylene have been proposed, including the propane dehydrogenation (PDH), the methanol–olefin process and the Fischer–Tropsch olefin process [2]. The development of shale gas [5] extraction methods has generated an abundance of light alkanes, therefore making propane dehydrogenation the best candidate for replacing conventional propylene production processes [6]. Several catalysts and propane dehydrogenation processes have been developed, whose representatives are UOP Oleflex, Lummus Catofin, Linde–BASF PDH, Uhde STA and Snamprogetti–Yarsintez FBD [2]. Currently, Lummus Catofin [7] and UOP Oleflex [8] are mainly used in industrialized devices. The Catofin process uses chromium/aluminum-based catalysts, which show good performance, assuring good stability and high propylene yield and resulting in a propylene selectivity higher than 87% [2]. However, this process has low efficiency due to frequent switching to high-temperature conditions [2]; moreover, chromium is not considered an environmentally friendly catalyst. The Oleflex process uses platinum/aluminum-based catalysts, and the hydrogen produced together with propylene can be used as fuel in the unit; furthermore, the dehydrogenation unit can be integrated with downstream conversion processes [2]. At the moment, therefore, processes using

platinum-based catalysts can provide the highest propylene selectivity, high reaction rate and stability and can be considered more eco-friendly than chromium-based ones. In this review article, a selection of the most recent and relevant articles published in the last three years (2019–2021) on platinum-based catalysts are reviewed, focusing on how both promoters and supports may affect the catalytic activity in terms of deactivation resistance. Although in most cases it is difficult to make a clear distinction between articles dealing with bimetallic systems and support effect, the distribution of articles between sections and paragraphs has been made on the basis of the main conclusions reported in the articles themselves. Furthermore, at the end of the main sections or paragraphs, a summary of the results is provided. Finally, one section focuses exclusively on theoretical studies, while the last two sections focus on some relevant studies on reactor configuration and catalyst regeneration.

2. The Reaction

Propane dehydrogenation is an equilibrium endothermic reaction (1). The thermodynamic analysis shows that the equilibrium conversion drops exponentially with pressure, so a reduction in hydrocarbon partial pressure can be beneficial to increase the conversion [9]. To reduce the hydrocarbon partial pressure, steam or other inert gases can be used to dilute the reacting mixture; steam is preferred to compensate for the conversion decrease, but an increase in reaction temperature is necessary [9]. Therefore, to obtain high propane conversions, high operating temperatures (800–950 K) are required.

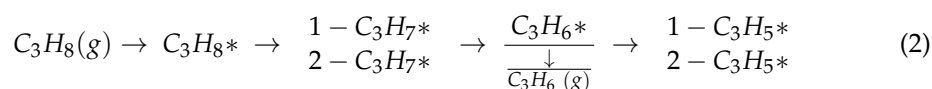


The reaction conditions therefore result in an increase in side reactions such as thermal cracking, deep dehydrogenation, coke formation and the sintering of the supported nanoparticles, limiting the average life of the catalyst [6]. To overcome the catalyst deactivation, it is therefore mandatory to employ a periodic regeneration through oxidative cycles to eliminate the coke, followed by reduction; moreover, oxygen–chlorine treatment can be carried out to partially redisperse agglomerated Pt particles [10].

The side reactions are attributed to the persistence of propylene on the active site; therefore, the geometric and the electronic features of the catalysts play a crucial role in the suppressing of them [2].

Moreover, the propylene formation rate and the selectivity–conversion relationships for propylene and coke formation depend on the kind of supported metal, on the loading, on the size of supported metal nanoparticles, on the presence of promoters and on the reaction temperature [11].

Recently, a study was published on the dependence, in Pt/Al₂O₃ catalysts, between the catalytic performance and the Pt particle size [12]. The results showed that the turnover frequency decreases with the increase in the particle size, and the atomically dispersed catalysts exhibited a turnover frequency 7-fold higher than that of the nanoparticles. Concerning the propylene selectivity, a canyon shape dependence was observed, with a bottom around 2 nm of the particle size; the net of the two trends demonstrates that the atomically dispersed species can provide higher propylene yields thanks to a reduced permanence of the reactive species on the catalytic site, thus preventing deep dehydrogenation and cracking.



In Figure 1 a schematic representation of the main steps in PDH reaction is shown, which can be summarized in four steps (2), namely C–H activation of propane molecules, cracking, desorption of propylene and deep dehydrogenation of propylene, which are regulated by the effects of promoters and supports on the adsorption of the propyl intermediate [2]. Theoretical and experimental studies have demonstrated that Pt⁺ cations promote the propane dehydrogenation to give the corresponding [Pt + propylene]⁺ and

[Pt + propyne]⁺ [13]. Moreover, Pt–Pt ensembles seem to be responsible for the propylene deep dehydrogenation and hydrogenolysis, so the insolation of Pt atoms could be an effective strategy to inhibit the side reactions [14]. In this regard, single-atom Pt has been enclosed in thermally stable intermetallic PtGa, in which the three-fold-Pt ensembles are deactivated by Pb deposition. The resulting PtGa-Pb/SiO₂ catalyst exhibited a propane conversion of 30%, a propylene selectivity of 99.6% at 873 K and stable performance for 96 h [14]. Reduction temperature seems to play a crucial role in Pt/CeO₂ catalysts; reduction at 1248 K leads to low reaction rates, while a reduction temperature of 823 K allows high propylene selectivity [15]. It is interesting to note that the type of salt precursor of the active phase may also have a role in catalyst performance. Supported Pt–Sn catalysts are conventionally prepared by using Cl-containing precursors, such as SnCl₂ or SnCl₄; specific studies have demonstrated that the presence of chlorine may decrease the acidity, the specific surface area and pore volume of the catalyst and increase the mean pore diameter, thus affecting the selectivity [16]. However, to improve the coke resistance and prevent aggregation of active sites, generally, two main routes are served: the introduction of a second metal species, which can significantly favor the activity and stability of the Pt species, and, on the other hand, the use of supports with tuned acidic characteristics and preorganized structures, such as zeolite and hydrotalcite, that strongly interact with the active species. For example, the oxygen vacancies, in Al_{cu}–O Lewis acid–base pairs can be easily tuned through a CO reduction of the Al₂O₃ support [17]. It has been shown that adding a small amount of hydrogen to Pt–Sn/SiO₂ catalyst, in PDH reaction, effectively decreases the coke formation and improves the catalyst stability [18]. The addition of H₂ seems to help maintain the surface states of the active metals in the Pt–Sn/SiO₂ catalysts under the reaction conditions.

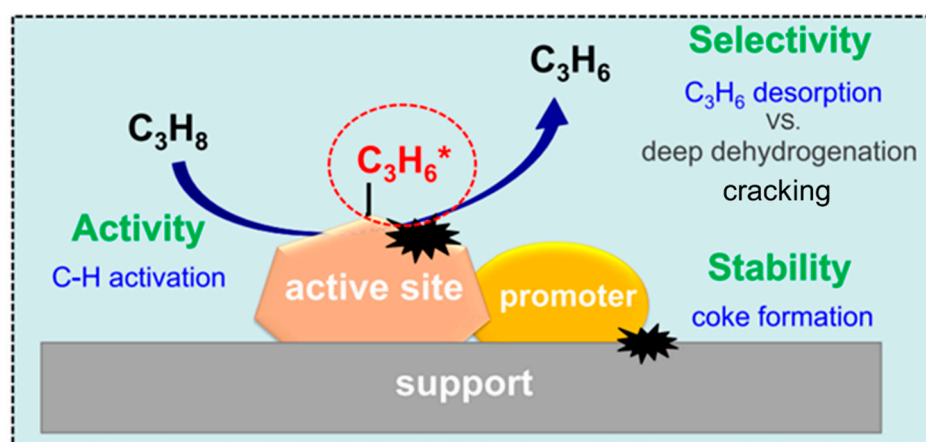


Figure 1. Schematic illustration of different steps during PDH reactions. Reprinted and modified with permission from ref. [2]. Copyright 2020 American Chemical Society.

3. Theoretical Studies

Several theoretical studies have recently been published on the use of platinum-based catalysts for the PDH reaction. The trends in the activity and selectivity for propylene production on a group of transition metals (Cu, Ag, Ni, Pt, Pd, Co, Rh, Ir, Ru, Re and Os) have been studied and parameterized as a function of two relevant C₃ descriptors (CH₃CHCH₂ and CH₃CH₂CH) [19]. The simulation clearly showed that Pt is the only pure metal catalyst with good activity and propylene selectivity in PDH reaction.

Among the bimetallic catalytic systems, the Pt–Sn has been extensively studied through density functional theory (DFT) calculations. The reaction pathway for Pt–Sn catalytic systems was studied, demonstrating that a single Pt site can break the propane C–H bond; moreover, the interface and Sn can increase the catalyst stability and suppress the deep dehydrogenation [20]. Compared to the monometallic Pt catalyst, the Pt–Sn bimetallic catalysts showed improved turnover rates, propylene selectivity and stability in PDH

reaction [21]. The high turnover rates are attributed to the electronic effects that weaken Pt-hydrocarbon chemisorption energies. Moreover, the turnover rate increases with the Pt-Sn coordination number, while the higher propylene selectivity was attributed to the geometric effects of Sn in reducing the Pt ensembles. The energy required for Sn atoms to move from the bulk to the surface in a $\text{Pt}_3\text{Sn@Pt}$ model was calculated, demonstrating that the most negative segregation energy happens with a Pt_3Sn top layer and four Sn atoms at the surface [22]. Moreover, it has been demonstrated that the Pt_3Sn alloy surface can be easily restored by reduction after an acid etching controlled process, showing that the Pt_3Sn alloy surface is recoverable and thermodynamically preferable.

Other effective bimetallic catalytic systems have been studied, such as the PtZn_4 surface, whose geometric and electronic structures activate the first and second C–H bonds of propane but inhibit the coke formation [23]. The Pt electronic features on boron nitride nanosheets can be adjusted by rational deposition on the support so that different charge states show different catalytic performances in PDH reaction [24]. Calculations demonstrate that Pt supported on boron vacancy is more reactive towards propane, propene and hydrogen adsorption and has a lower energy barrier for deep dehydrogenation of propene than Pt supported on nitrogen vacancy (Figure 2).

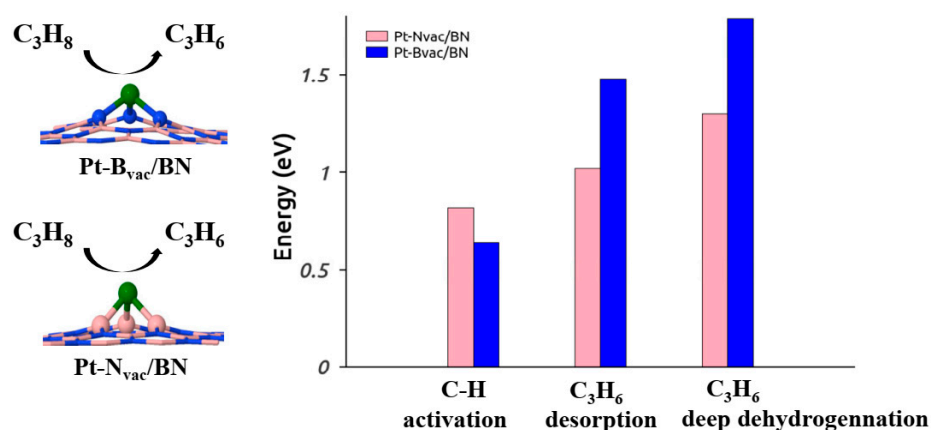


Figure 2. Comparison of energy barriers for C–H activation, C_3H_6 desorption and deep dehydrogenation on boron (Bvac) and nitrogen (Nvac) vacancies. Reprinted with permission from ref. [24]. Copyright 2021 Elsevier.

The addition of boron, before platinum loading on $\gamma\text{-Al}_2\text{O}_3$ support, gives rise to a promotion effect by reducing carbon deposition and enhancing the propylene selectivity in PDH reaction [25]. DFT calculations showed that the boron promotion is realized through the formation of amorphous oxide both on the support and on the platinum particles.

The studies on Co@Pt catalyst have shown that the core–shell system is catalytically less active than Pt but shows higher propylene selectivity as the result of less negative propylene adsorption energies and higher activation energies in the PDH reaction [26].

The addition of vanadium to platinum results in the formation of the Pt_3V intermetallic compound with a structure like AuCu_3 , which shows the same catalytic performance of an alloy surface layer on a Pt core [27]. A change in the orbital energy in Pt–V alloys causes the weakening of the adsorbate bonding to the Pt, leading to a more stable binding geometry.

A comparison between the performance of MgO-supported Pt_3 and Pt_7 with Pt_2Ge and Pt_7Ge has shown that Ge is a good dopant to regulate Pt selectivity [28]. Alloying Pt with Ge reduces the affinity between the pure metallic clusters and alkenes, thus favoring the alkene desorption; moreover, for the smallest PtGe clusters, the sintering by Ostwald ripening is less likely. The presence of Ge reduces the carbon affinity, thus improving the resistance to coke formation.

As we discuss afterward, one strategy to improve the selectivity of the catalysts in PDH reaction is to trap the metal clusters in the zeolites to suppress sintering. However, a significant passivation effect of the surrounding zeolite structure on the center of the d-

band and on the catalytic performance of closed Pt clusters has recently been reported [29]. The zeolitic framework suppresses the propylene desorption, decreasing the selectivity and increasing the coke deposition, thus making the zeolitic environment surrounding not beneficial for PDH reaction.

Platinum has also been studied as a dopant in Cr_2O_3 and ZnO catalytic systems for PDH reaction [30]; in the case of chromium oxide, the Pt doping affects the physiochemical properties of close oxygen atoms and lowers the activation energy for rate determination. In the case of ZnO , the Pt doping can speed up the H diffusion, stabilize the H atoms and promote the H_2 desorption.

Combining microkinetic analysis and DFT calculations, a Pt-doped Ga_2O_3 catalytic system was studied, and its bifunctional character was demonstrated [31]. At the $\text{Ga}(\text{o})\text{-O}$ site, a Lewis acid–base interaction occurs when a pair of H atoms can be coadsorbed at the $\text{Ga}(\text{o})$ and O ion pair, thus providing a positive effect on hydrogen recombination. The Pt–O site is more active than the $\text{Ga}(\text{o})\text{-O}$ site in the propane activation, having a lower activation energy of the rate-limiting step. However, further studies have demonstrated that the $\text{Ir}_1\text{-Ga}_2\text{O}_3$ catalyst is more effective than the Pt-doped Ga_2O_3 catalyst in PDH reaction [32].

In summary, in this section, a series of theoretical studies focus on the promoted and bimetallic systems. Although platinum itself is active in the dehydrogenation reaction of propane, the presence of promoters or bimetallic systems in general provides better performance in terms of stability. These results are essentially attributed to the electronic effects due to the formation of metal alloys. Interestingly, the possibility of trapping metal species in a preorganized structure, such as a zeolite, can be detrimental in the desorption of propylene, thus reducing the stability of the catalyst. As we will see later, a series of experimental articles seem to contradict these results, making further investigation urgent.

4. Polymetallic and Promoted Catalysts

This section reports the main results claimed by a series of articles focusing on bi- and polymetal promoted systems; for clarity, a summary table is provided at the end of the section, which summarizes the best results in terms of yield and selectivity for propylene and deactivation rate.

Several bimetallic catalytic systems have been studied, including Pt–Sn, Pt–Co, Pt–Ge, Pt–Zn and so on. Synthetic methodology and characterization are crucial steps toward understanding structure–activity relationships in PDH bimetallic catalysts [33]. The most used preparation method is impregnation followed by reduction, with the aim to obtain an alloy. Recently, colloidal methods to obtain supported Pt–In and Pt–Ga nanoparticles have been reported, displaying uniform phases, ensuring that promoter atoms are fully incorporated into the bimetallic nanoparticle and no excess promoter oxide remains on the surface [33].

4.1. Bimetallic and Promoted Catalysts

The effect of different promoters, including Ce, In, La and Fe, was evaluated with Pt/Sn-SBA-15 catalyst, in which Sn was used as dopant for SBA-15 [34]. The addition of promoters affected the reducibility, acidity, surface content and stability of metallic Pt particles and the coke formation. The FePt/Sn-SBA-15 catalyst showed the best initial propane conversion; on the other hand, the InPt/Sn-SBA-15 catalyst exhibited the best performance in time on stream test (Figure 3). Indium promoted the formation of surface Pt oxides and their reduction; moreover, it stabilized the metallic Pt under the reaction conditions. Indium and platinum oxides were partially reduced, suggesting that oxygen vacancies can be generated during the reaction.

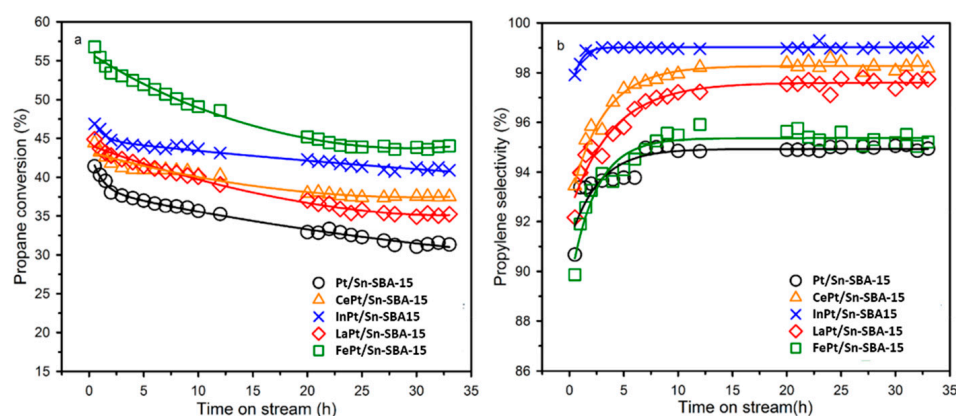


Figure 3. Comparison between the conversion (a) and propene selectivity (b) of promoted MPt/Sn-SBA-15 (M = Ce, In, La, Fe) (reaction conditions: $C_3H_8/Ar = 1/4$, $WHSV = 4.05\ h^{-1}$, 853 K). Reprinted with permission from ref. [34]. Copyright 2019 American Chemical Society.

Pt-Sn is one of the most promising catalytic systems, the performance of which is strongly dependent on its structure. Sn can promote the separation of multifold Pt sites and donate electrons to Pt; comparative studies between Pt/ Al_2O_3 and PtSn/ Al_2O_3 highlight, in the case of bimetallic catalyst, a significantly higher propylene selectivity and only traces of cracking products [35]. In fact, the multifold Pt (111) sites are more active towards the breaking of C–C bonds than the PtSn (102).

Two critical parameters are involved in the preparation of these catalysts, namely the particle size and the making of a Pt-Sn alloy, to enhance the synergy effect between the two metals. A novel grafting approach, using surface organometallic chemistry, has been developed for the synthesis of Pt-Sn bimetallic clusters (around 0.75 nm) with an alloy structure on the surface of $\theta-Al_2O_3$, which showed superior performance with respect to the corresponding impregnated catalyst [36]. A mixture of PtSn and Pt_3Sn alloys was also obtained by direct reduction method, i.e., without conventional calcination, of Pt-Sn/ Al_2O_3 catalyst [37]. Good performance has also been reported with Pt_1Sn_1/SiO_2 catalysts, in which the interaction with the support prevents the Pt-Sn segregation and formation of a tin oxide phase [38].

The Pt-Co catalysts show much higher propylene selectivity than the monometallic Pt or Co in the PDH reaction [39]. The turnover rates of Pt in the bimetallic catalysts are similar to monometallic Pt, thus suggesting that the active sites are the resulting alloys. The Co acts as a nonactive promoter, and thus the high selectivity of Pt_3Co can be attributed to geometric effects, due to the presence of smaller Pt–Pt ensembles, and to the decrease in the energy of the Pt 5d orbitals compared to monometallic Pt.

A Ge-promoted Pt catalyst has been developed, showing outstanding stability in comparison to the monometallic Pt/ Al_2O_3 catalyst [40]. The Pt-Ge alloy formation allows the dilution of Pt surface, breaking the Pt ensembles and withdrawing electrons from Pt, which inhibits the C–C bond cleavage, the hydrogenolysis and the coke formation, thus obtaining enhanced propylene selectivity.

Both DFT calculation and experimental results demonstrated that the formation of PtMn alloy nanoparticles on the SiO_2 -based support increases the electron density of Pt due to the electron transfer from Mn to Pt [41]. The Mn doping is able to improve the dispersion and stabilize the Pt clusters, thus improving the performance in PDH reaction.

Zeolite-stabilized Pt-Zn catalysts, in which Zn species are stabilized by silanols from dealumination of the zeolite structure, act as anchor sites for Pt species [42]. Pt-Zn species are highly dispersed on the support surface; the two metals are in close contact, and strong electronic interaction is guaranteed. The 0.1Pt-2Zn/Si-beta catalyst showed high propylene production rate and selectivity and a sustainable deactivation rate during the PDH reaction. The coke deposition was very low; therefore, the irreversible deactivation of the catalyst was attributed to the loss of Zn species and the consequent aggregation of Pt species. Of

great interest is the 10Zn0.1Pt/HZSM-5 catalytic system, the good performance of which has been attributed to the presence of two kinds of active centers that work corporately, Lewis acidic sites created by Zn framework species and small-sized PtZn particles [43]. Similarly, the titanium framework of the titanium silicon zeolite TS-1 is able to localize Pt and Zn together, in PtZn/TS-1 catalyst, by increasing the dispersion of Pt and improving its modification by Zn [44].

Atomic layer deposition (ALD) has been used to tailor the interface between Pt nanoparticles and the SiO₂ support [45]; the SiO₂ surface was modified by homogeneous deposition of a thin ZnO layer, and the resulting support was impregnated with platinum precursor. Reductive thermal treatment gave rise to a phase transformation to form Pt₁Zn₁ alloy nanoparticles. The resulting catalyst showed higher activity than the corresponding catalyst prepared by incipient wetness impregnation. The nanoalloy formation induces electronic and geometric modification of Pt, which reduces side reactions.

4.2. Supported Liquid Metal Solutions

Liquid metal catalysts do not have some of the problems of heterogeneous catalysts, such as the presence of different active centers, i.e., defects and irregularities of the solid surface [46]. In the case of the liquid metal solution, the active metals are in a uniform steric and electronic environment. However, they may suffer from stability problems at high temperatures, and the separation of the reaction products from the catalyst is sometimes difficult to accomplish. The possibility of supporting these catalysts on solid porous supports, to obtain the so-called supported catalytically active liquid metal solutions (SCALMS), allows merging the positive features of both heterogeneous and molecular catalysis. The key difference, with respect to the conventional intermetallic compounds, is the low melting temperature of the system. Under dehydrogenation conditions (>623 K) the Ga/noble metal phase is present as a homogeneous liquid [47]. Diffuse reflectance infrared Fourier transform spectroscopy (DRIFTS), with CO as a probe molecule, has been applied to Ga/Al₂O₃, Pt/Al₂O₃ and Ga₃₇Pt/Al₂O₃ catalysts to investigate the nature of the active Pt species, demonstrating the presence of isolated Pt atoms on the liquid SCALMS surface [47]. Under operando conditions, during PDH in CO/propane and in Ar/propane, Pt/Al₂O₃ sample is rapidly poisoned by CO adsorption and coke formation, while no poisoning was observed over Ga₃₇Pt/Al₂O₃. Ga/Al₂O₃ is more active than Pt/Al₂O₃ due to the presence of Ga⁺ species on the surface of the catalyst. IR spectra and DFT studies suggested that the Ga matrix and the presence of coadsorbates modify the electronic properties of the surface Pt species.

Spatially resolved kinetic data were acquired during PDH over GaPt/SiO₂ SCALMS [48]. The results showed an enhanced deactivation of the catalyst at the end of the bed, with the deactivation front moving from the end to the beginning of the catalyst bed over the time on stream, probably due to the enhanced coking of the catalyst under high conversion.

4.3. Polymetallic Catalysts

Polymetallic catalysts have also been studied, such as K-PtSn/Al₂O₃ [49] and Ce, Zn and Co (0.3, 0.5 and 0.7 wt%) promoted trimetallic Pt-Sn-K/Al₂O₃ catalysts for PDH reaction [50]. The results highlighted the superior promoting effect of Ce; the Pt–Ce interactions could prevent the Pt particle agglomeration, and Ce could promote the thermal stability of γ -Al₂O₃. The synergic effect of Co and Zn can enhance the Pt reducibility and consequently suppress the coke formation.

Lanthanum was used to improve the performance of PtSn/ γ -Al₂O₃ catalyst; the parent catalyst was impregnated with different amounts of lanthanum salt precursor to obtain a loading of 0, 1.2, 2.2 or 3.2 wt% [51]. La can improve both propane conversion and propylene selectivity, and the best performance was obtained with a loading of 2.2 wt%.

Ca and Pb have been used to modify the geometric and electronic features of PtGa/SiO₂ catalyst by decorating the PtGa nanoparticles on silica support [52]. Lead was deposited on the three-fold Pt and Ga sites of the PtGa nanoparticles to block the Pt₃ sites, thus favoring

the dehydrogenation and inhibiting the deep dehydrogenation. Due to the atomic size, lead does not diffuse into the structure, even at high temperatures, thus providing stability. Calcium, which has been added around the PtGa nanoparticles, acts as an electron donor agent to provide an electron-enriched Pt1 site, highly selective in PDH reaction (Figure 4).

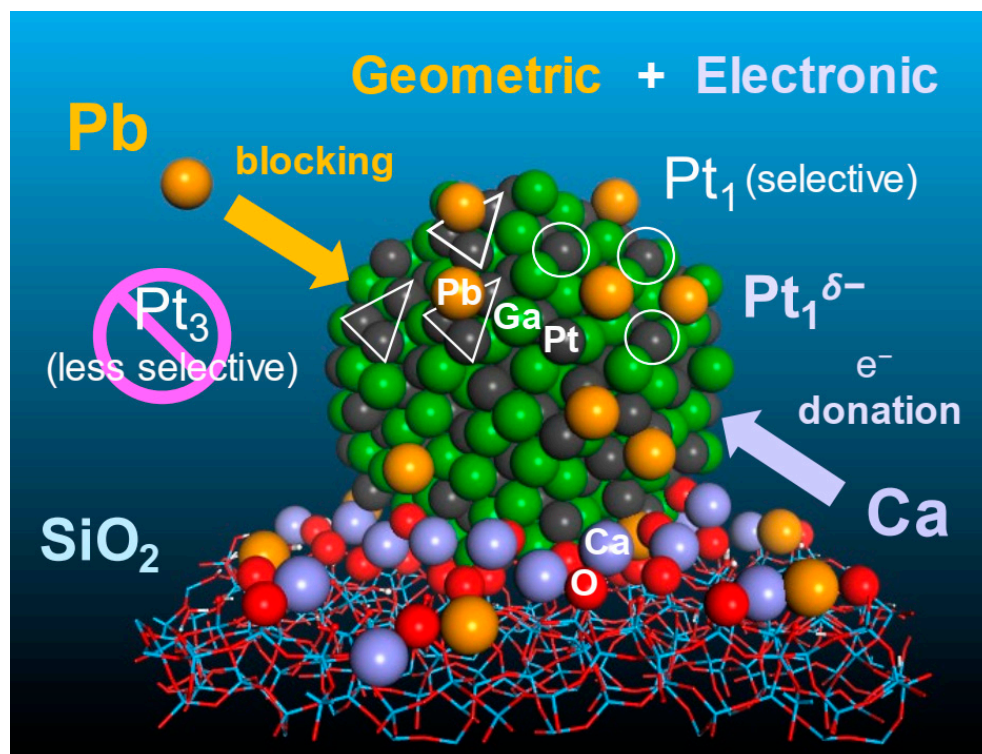


Figure 4. Catalyst design concept for the double decoration of the nanoparticulate intermetallic PtGa-CaPb/SiO₂. Reprinted with permission from ref. [52]. Copyright 2021 Wiley-VCH GmbH.

In summary, in this section, the results of a series of articles focused on the use of bi- and polymetal systems have been reviewed. As highlighted in the section dedicated to theoretical studies, the improvement in performance is attributed to electronic effects. The data summarized in Table 1 show that the best performances in terms of propylene selectivity and yield, as well as the deactivation rate, are obtained with platinum/tin-based catalytic systems, in one case promoted by indium. The data on catalytic systems based on platinum/zinc and platinum/gallium are contrasting, as their performances seem dependent on the reaction conditions.

Table 1. Polymetallic and promoted catalysts: reaction conditions, propylene selectivity, propylene yield and deactivation rate per selected catalyst of each article.

Catalyst	Reaction Conditions	Reactor	Time on Stream Test	Propylene Selectivity (S) and Yield (Y)	Deactivation Rate ^a	Ref.
InPt/Sn-SBA-15	C ₃ H ₈ /Ar = 1/4 WHSV = 4.05 h ⁻¹	Fixed bed i.d. = 10 mm l = 200 mm	1 atm 853 K 33 h	S = 99% Y = 40.5%	0.007 h ⁻¹	[34]
Pt-Sn _{3.00} /θ-Al ₂ O ₃	C ₃ H ₈ /H ₂ /He = 1/1/8 WHSV = 11.8 h ⁻¹	Fixed bed -	1 atm 823 K 24 h	S = 99% Y = 37.6%	0.009 h ⁻¹	[36]
Pt-Sn/Al ₂ O ₃	C ₃ H ₈ /H ₂ /N ₂ = 3/3/7 WHSV = 8.9 h ⁻¹	Fixed bed i.d. = 18 mm	1 atm 873 K 5 h	S > 94% Y = 29.7%	0.083 h ⁻¹	[37]
Pt ₁ Sn ₁ /SiO ₂	C ₃ H ₈ = 1 WHSV = 4.7 h ⁻¹	Packed bed i.d. = 7 mm	1 atm 853 K 30 h	S > 99% Y = 38%	0.003 h ⁻¹	[38]
Pt _{0.5} -Ge _{1.5} /Al ₂ O ₃	C ₃ H ₈ /H ₂ /N ₂ /Ar = 1/1.5/18/24/1	Fixed bed i.d. = 5 mm l = 600 mm	1 atm 873 K 250 min	S = 97.2% Y = 51.4%	0.10 h ⁻¹	[40]
Pt/0.5Mn-DMSN	C ₃ H ₈ /N ₂ = 1/2 WHSV = 2.4 h ⁻¹	Fixed bed -	863 K 100 h	S > 99% Y = 40.1%	0.007 h ⁻¹	[41]
0.1Pt-2Zn/Si-beta	C ₃ H ₈ /He = 1/9 WHSV = 2.4 h ⁻¹	Fixed bed i.d. = 6 mm	1 atm 823 K 150 h	S = 98% Y = 36%	0.008 h ⁻¹	[42]
10Zn0.1Pt/HZ	C ₃ H ₈ /N ₂ = 5/95 WHSV = 0.24 h ⁻¹	Fixed bed i.d. = 6 mm	1 atm 798 K 65 h	S = 93% Y = 40%	0.008 h ⁻¹	[43]

Table 1. Cont.

Catalyst	Reaction Conditions	Reactor	Time on Stream Test	Propylene Selectivity (S) and Yield (Y)	Deactivation Rate ^a	Ref.
PtZn/TS-170	C ₃ H ₈ = 1 WHSV = 12 h ⁻¹	Fixed bed -	1 atm 873 K 97 h	S > 96% Y = 19.7%	0.0158 h ⁻¹	[44]
PtZn/SiO ₂	C ₃ H ₈ /He = 2/8 GHSV = 6000 mL g ⁻¹ h ⁻¹	Fixed bed i.d. = 10 mm	1 atm 873 K 12 h	S = 97% Y = 47.5%	0.0133 h ⁻¹	[45]
Ga-Pt SCALMS	C ₃ H ₈ /He = 3/22 WHSV = 1.4 h ⁻¹	Compact Profile Reactor (CPR) i.d. = 4 mm o.d. = 6 mm l = 180 mm	773 K 15 h	S ≈ 100% Y = 8%	0.064 h ⁻¹	[48]
Pt-Sn-K-Co _{0.3} -Zn _{0.7} /γ-Al ₂ O ₃	C ₃ H ₈ /H ₂ = 1.2/1 WHSV = 2 h ⁻¹	Fixed bed i.d. = 15 mm	1 atm 893 K 10 h	S = 90% Y = 39.6%	0.024 h ⁻¹	[50]
Pt-Sn-La(2.2)/Al ₂ O ₃	C ₃ H ₈ = 1 WHSV = 1.9 h ⁻¹	Fixed bed i.d. = 18 mm	1 atm 873 K 13 h	S = 84.6% Y = 29%	0.042 h ⁻¹	[51]
PtGa-CaPb/SiO ₂	C ₃ H ₈ /H ₂ /He = 2.5/1.25/3.75 WHSV = 5.9 h ⁻¹	Fixed bed i.d. = 8 mm	1 atm 873 K 720 h	S > 99% Y > 30%	0.00033 h ⁻¹	[52]

$$^a k_d = \frac{\ln\left(\frac{100-X_{end}}{X_{end}}\right) - \ln\left(\frac{100-X_{in}}{X_{in}}\right)}{t}; [40].$$

5. The Effect of the Support

This section reports the main results claimed by a series of articles focused on the effect of the support; a summary table is provided at the end of the section to summarize the best results in terms of propylene yield and selectivity and deactivation rate.

The surface and textural properties of the catalyst support have a crucial role in regulating the catalytic performance of the catalysts. Specific surface area, acid–base properties, shape and thermal stability may have significant influences on the catalytic performance of Pt-based catalysts [53]. Alumina is the most used support [54]; it was shown that the unsaturated coordinate Al^{3+} sites (penta-coordinated Al^{3+} , $\text{Al}^{3+}_{\text{penta}}$) play a crucial role in the PDH activity of the Pt/Ga/ Al_2O_3 catalysts [55]. $\text{Al}^{3+}_{\text{penta}}$ sites are able to promote the dispersion of Pt and Ga ions on the Al_2O_3 support, thus facilitating the effective hydrogen spillover between Pt and Ga and generating hydrogen desorption from the active sites of Ga_2O_3 . Highly ordered mesoporous Al_2O_3 supports, with different levels of $\text{Al}^{3+}_{\text{penta}}$ sites, have been prepared and tested to disperse Pt-Sn₂ clusters via a formation of Al–O–Pt bonds, thus preventing the agglomeration of the clusters [56].

5.1. Support Acid–Base Properties

As already mentioned, the regulation of the acid–base properties of the support can be fundamental to prevent side reactions and coke formation. Direct evidence of the relation between Lewis acid sites and coke formation, in alumina-based catalysts, has been demonstrated; in fact, the reduction of the strong Lewis acid sites leads to suppression of metal sintering and coke formation [57]. The effect of physically adding nanostructured metal oxides TiO_2 , ZrO_2 and Al_2O_3 to Pt-Sn/ γ - Al_2O_3 catalysts in PDH reaction at 823 K was investigated [58]. The additives did not affect the performance of the catalysts but markedly enhanced the catalyst stability, in terms of less coke formation (both aliphatic and aromatic), with a decrease by approximately 3%, 19% and 32% in presence of Al_2O_3 , ZrO_2 and TiO_2 , respectively. These results were explained in terms of the number of oxygen vacancy defect sites, which are involved in the adsorption of coke precursors generated on Pt particles, in that a decrease in coke formation on Pt-Sn/ γ - Al_2O_3 catalyst corresponds to an increase in the coke deposition on the acidic sites of the additives. The effect of different percentages of TiO_2 in $\text{TiO}_2\text{Al}_2\text{O}_3$ support (AT_n , $n = \text{TiO}_2/(\text{Al}_2\text{O}_3 + \text{TiO}_2) = 0\text{--}100$), in Pt-Sn/ $\text{TiO}_2\text{Al}_2\text{O}_3$ catalysts, has been investigated, showing that the addition of TiO_2 can regulate the acid properties of the composite support and promote the metal–support interactions [59]. The best performance was obtained with PtSn/ AT_{20} catalyst; the proper acidity prevents the coke formation and side reactions, and enhanced metal support interactions improve the dispersion of PtSn on the support and prevent the Pt aggregation.

Calcium has been reported to promote the catalytic activity of $\text{Pt}_{0.5}\text{-Ge}_{1.5}/\text{Al}_2\text{O}_3$ in the PDH reaction, in terms of higher propylene selectivity and lower coke formation, thus improving the stability as the result of the suppression of the strongest acid sites [60].

The aging temperature in the alumina preparation has a significant effect on the physical and chemical properties of the support [61]. The increase in the aging temperature led to an increase in the pore size and the pore volume; moreover, the pore size distribution became broader due to the boehmite phase formation and to needle or rod-like alumina structures formed after calcination. The aging temperature also has an influence on the surface properties of the PtSnK/ Al_2O_3 catalyst. By increasing the aging temperature, the dispersion of Pt and the total acid content of the catalyst increase until reaching a maximum, located between 423 and 523 K, and then decrease with the temperature. Moreover, an increase in the aging temperature enhances the interaction between SnOx and the support, thus inhibiting the reduction and reducing the Sn⁰ formation.

The Lewis acid sites of beta zeolites can improve the conversion by increasing the metal dispersion, while Brønsted acid sites can catalyze the cracking reactions, oligomerization and aromatization [62]. When comparing the performance of the Pt-Sn/beta catalysts ($\text{SiO}_2/\text{Al}_2\text{O}_3 = 38$ or 300), the Pt-Sn/beta catalyst (300) showed the best catalytic activity of PDH despite the lower dispersion of Pt [62].

The dealumination of zeolites allows the decrease in the acidity of the support and the incorporation of Sn atoms into the zeolite (BEA, SiO₂/Al₂O₃ ratio of 25) framework [63]. The corresponding Pt-Sn/zeolite catalysts show a Pt-Sn interaction that provides high selectivity and an increase in the agglomeration resistance of the active phase.

Titanium-based zeolite TS-1 has been enwrapped with SBA-16 silica to obtain a composite material to use as support for Pt-Sn-based catalysts [64]. Comparing the effect of different percentages of TS-1 (0–20%), the best performance in PDH reaction was obtained with the amount of 10% in the composite. The catalytic performance of Pt-SnO_x/TS-1@SBA-16 was interpreted as the result of the synergistic effect in the effective mass transfer through the hierarchical porous structure of the suited acidity and of the electronic effect of Ti species, which stabilizes the SnO_x species.

Three different pH values (9–11) were used for the synthesis of Boron-modified ZrO₂ (B-ZrO₂), subsequently adopted as the supports of PtSn catalysts (PtSn/B-ZrO_{2-x}); the characterization results showed that the acid strength increased with the synthesis pH [65]. In particular, the moderate interaction occurring between the metal species and B-ZrO₂-10 support results in a stronger interaction between Pt and Sn. In this way, the migration of coke precursor from the active sites to the support is facilitated, resulting in better stability in PDH conditions.

5.2. Support Morphology

In order to suppress aggregation, metal leaching and sintering during high-temperature reactions, supports with different morphologies have been studied. Sub-nanometric metal species show unique catalytic behavior compared to their nanoparticulate counterparts. However, the poor stabilization of these species towards sintering at high temperatures, under oxidative or reductive reaction conditions, limits their catalytic application.

The strong metal–support interactions (SMSIs) are defined as an encapsulation of the metal nanoparticles by the oxide over layers, blocking access to the nanoparticle surface [66]. SMSI encapsulation is performed by reducing substoichiometric oxide supports, which migrate over the metal nanoparticles. Good examples are Pt-Ti/SiO₂ and Pt-Nb/SiO₂ catalysts, obtained by impregnation of organometallic precursors, which showed SMSI behaviors [66]. Partial covering of the catalytic surface by the SMSI oxides resulted in lower activity per gram of Pt but similar TORs in PDH reaction; however, higher selectivity for propylene was obtained.

Highly stable and active Pt and Pt-Sn sub-nanometric clusters can be located in sinusoidal zeolite channels (pure-silica MFI), obtaining improved performance in PDH reaction [67,68]. Pt-Ni alloy nanoparticles have been encapsulated in perovskite-type oxide [69]. The appropriate amount of Pt, which is optimal to be confined in the lattice and to obtain the Pt-Ni alloy sites with moderate Pt-Ni interaction, was found to be 0.4%. The confinement has been shown to be crucial to enhance the propane conversion and the propene selectivity. Dealuminated H β (SiO₂/Al₂O₃ = 25) was used to encapsulate Sn species existing in tetrahedral coordination states into the framework of dealuminated beta (Si-beta) [70]. The strong Pt-Sn (IV) interactions inhibited the coke formation, while high dispersion of the ultrasmall nanoclusters inhibited the sintering of Pt clusters [71].

Stabilized Pt-Zn/Si-beta catalyst has been prepared by dealumination followed by Zn stabilization by the silanol defects of the zeolite framework, which then act as the anchoring sites for Pt species [42]. The resulting catalyst showed high propylene production rate and selectivity, and the irreversible deactivation was attributed to the loss of Zn species, which led to the Pt aggregation at high temperatures. Similarly, ultrasmall PtZn bimetallic nanoclusters have been encapsulated in silicalite-1 zeolite (S-1) (Figure 5), thus obtaining a highly active and selective catalyst for propane dehydrogenation [72]. The introduction of Cs⁺ ions into the zeolite is able to improve the regeneration of the catalyst, without affecting the catalytic activity [73].

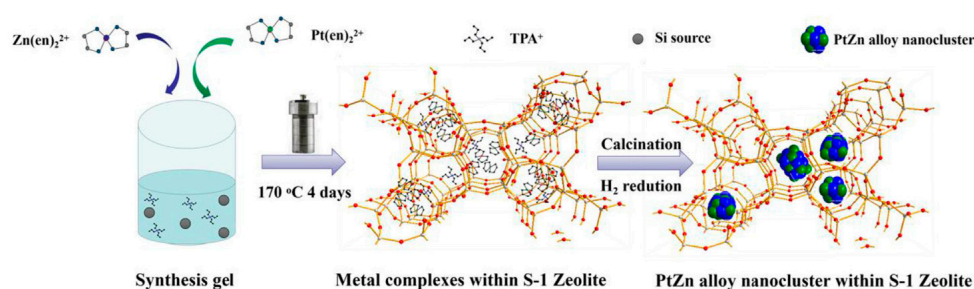


Figure 5. Illustration of the preparation of PtZn@S-1 catalyst. Reprinted with permission from ref. [72]. Copyright 2021 Elsevier.

Various metals have been used to dope silicalite-1 (M-S1, M = Mg, Al, Fe and In), and the corresponding PtSn/M-S1 catalysts showed the micro- and mesoporous hybrid structure feature [74]. The addition of the metal elements significantly affected the catalyst acidity and reducibility, increasing the hydrogen consumption due to the enhanced reduction of Pt and Sn oxides. The addition of Mg increased the stability, while PtSn/Fe-S1 showed the best initial activity in the PDH reaction.

Silicalite-1 zeolite has been used to also encapsulate Ga-Pt nanoclusters; the resulting catalyst has shown enhanced activity and stability [75]. Moreover, the restriction of the zeolite structure seems to be able to enhance the regeneration stability of the catalyst, as the catalytic activity remained unchanged after four consecutive cycles. Similar results were obtained by encapsulating PtGa nanoparticles in MFI zeolite [76]. MFI was also used to obtain and confine intermetallic Pt1Zn1 alloy nanoparticles, which is promoted by the isolated silanols on the external surface of mesoporous zeolite [77].

Hierarchical structures and weakly acidic supports can improve the dispersion of Pt due to an increased metal–support interaction [78]. Promoter-free Pt on hierarchical silicalite-1 nanosheet shows high selectivity for propylene in PDH reaction. The hierarchical silicalite-1 nanosheet catalyst promotes the presence of small active Pt particles supported on silanol or defective surfaces of the hierarchical silicalite-1 nanosheet catalyst.

The properties of ZSM-5 zeolite with flower-shaped crystallites (ZFS) as a supporting material have been investigated in comparison with the traditional ZSM-5 zeolite [79]. The results showed that the pore structure in the ZFS was changed, and the acid content was decreased. In the corresponding PtSnNa/ZFS catalyst, the amount of oxidized Sn species was remarkably higher, and the dispersion of Pt improved; moreover, the coke deposits on PtSnNa/ZFS migrated from the active metals to the support, thus improving the stability.

Phosphorus-modified carbon nanotube-supported Pt nanoparticles have been used for the PDH process. The phosphorus modification improves the Pt dispersion, electron transfer or hybridization, stabilizing Pt nanoparticles to prevent agglomeration, thus enhancing the catalyst stability [80].

Peony-like coordinatively unsaturating pentahedral aluminum(III)-enriched alumina nanosheets were prepared by a glucose-assisted hydrothermal method and used as support for Pt-Sn-based catalysts [81]. The excellent catalyst stability has been attributed to the promoted mass transfer and coke precursor migration, due to the specific morphology. Moreover, the improved Pt sintering resistance was attributed to the stabilizing effect of the coordinatively unsaturating pentahedral aluminum(III).

Hexagonal boron nitride nanosheet supported Pt/Cu cluster catalysts are able to disperse and stabilize Pt/Cu clusters; the fault edges of the *h*-BN nanosheets and the strong interaction between Cu and B–O edge defects stabilizes the unique geometry and electronic state of the Pt/Cu clusters [82]. γ -Al₂O₃-supported Pt-In bimetallic catalysts, prepared by perovskite lattice interstitial confined reduction, have shown superior performance with respect to the industrial catalyst PtIn/ γ -Al₂O₃ in propane dehydrogenation [83]. The lattice interstitial confinement promotes the formation of small and highly dispersed Pt-In bimetallic species. The catalytic performance of these catalysts is regulated by the In³⁺/In⁰

ratio, the weak Pt-In interaction, the weakening of the surface acid sites and the sharing of the Al–O bond used to anchor the nanoparticles.

5.3. Mg(Al)O Support

Of great interest as a support is a hydrotalcite-like structure, layered magnesium–aluminum hydroxide, in which the addition of magnesium increases the basicity of the support and affects the mechanism of platinum complex anchoring during the synthesis of the supported catalysts [84]. Hydrotalcites are hydroxide layered structures. The heat treatment may change the structure of Mg–Al hydrotalcites from layered double hydroxide (LDH) to mixed metal oxide, by releasing water molecules from ca. 473 K and CO₂ from ca. 573 K, by carbonate decomposition. The original structure can be restored by rehydration, evidencing the presence of a mechanism of memory effect, while a further increase in the temperature (>1023 K) leads to a spinel structure (Figure 6) [85].

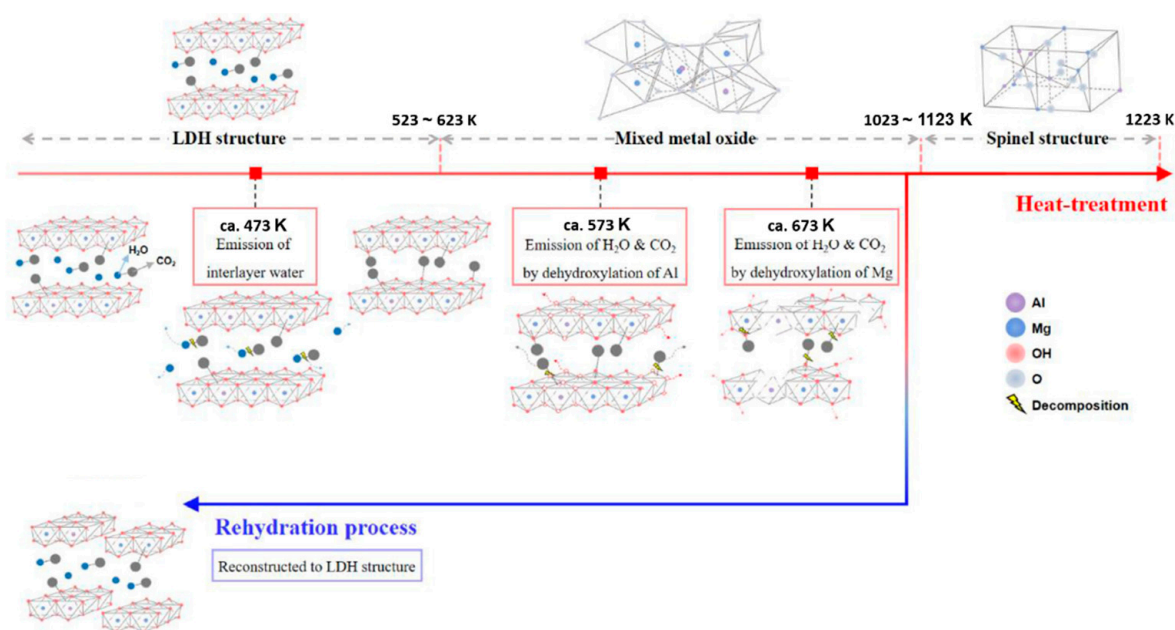


Figure 6. Schematic illustration of the structural changes in Mg–Al hydrotalcite during heat treatment and rehydration. Reprinted and modified with permission from ref. [85]. Copyright 2021 Elsevier.

The heat-treated hydrotalcite has strong surface base sites and good stability at relatively high temperatures, thus showing good performance in the case of reactions that requires strongly basic catalysts. The Sn-containing hydrotalcite was synthesized with variation of the tin content ($Mg/(Al + Sn) = 3$ and $Sn/(Sn + Al) = 0, 0.002, 0.005, 0.01, 0.05, 0.1, 0.3, 0.5, 0.7, 1.0$). The compound with $Sn/(Sn + Al) \leq 0.1$ ratio showed the formation of a system with uniform phase composition [86]. The introduction of Sn⁴⁺ cations in the hydroxide layers increases the positive charge of the layers and strength the electrostatic interaction with platinum in the catalyst, thus decreasing the mobility and preventing the formation of large platinum particles. The metal ions of Pt⁴⁺ and In³⁺ were introduced into the hydrotalcite layer during the reconstruction process [87]. The resulting ball-flower-like PtIn/Mg(Al)O catalyst, when used in the PDH reaction, showed very good performance in terms of activity, selectivity for propene and durability, as well as excellent resistance to coke deposition and Pt sintering. These results were attributed to the multilevel hierarchical microstructure; the lattice confinement of the reconstructed hydrotalcite-like precursor is able to stabilize the highly dispersed Pt species.

Comparative studies on the effect of the incorporation of Sn and In in Mg(Al)O on the stability of Pt/MgAl(X)O catalysts showed that the introduction of In gives rise to enhanced catalyst stability and propylene yield [88]. Close contact between Pt and well-dispersed InO_x species led to a promotional electronic effect, while Sn cations showed

a propensity to segregate on the support surface. The electronic modification of the Pt particles in the Pt/MgAl(In)O catalysts enhances the dehydrogenation activity and the anticoking capacity.

The addition of Zn to MgAlO layered double oxide support in PtSn-Mg(Zn)AlO catalyst has been studied, showing a promotional effect of Zn [89]. The addition of Zn can change the structure of the catalyst by changing the interfacial character between the metal particles and support, thus increasing the metal dispersion.

Au-Pt/MgAl layered double hydroxide catalysts have been extensively studied, showing that the anchoring of active metals complexes in the interlayer space of the support decreases the metal particle size and, as a consequence, improves the catalytic activity [90]. An increase in the Mg/Al ratio in the support leads to a decrease in the platinum dispersion; moreover, gold does not perform a dehydrogenating function, but the introduction of gold promotes the geometric dilution of platinum active centers, leading to an increased dispersion.

In summary, most of the articles published in the last three years on the dehydrogenation of propane in the presence of platinum-based catalysts focus on the effect of the support. The strategy is based on two main assumptions, namely regulating the surface acidity of the support to prevent the formation of coke and trapping the metal nanoparticles to avoid sintering. From the data summarized in Table 2 it is evident that the best performances were reported in the case of alumina-based substrate modified with calcium oxide and in the case of Si-beta zeolites obtained by dealumination. Concerning the latter case, theoretical studies have suggested that trapping structures can prevent the rapid desorption of propylene, thereby undermining the stability of the catalyst. On the contrary, the modification of the acid–base properties of the support seems to be a winning strategy in all cases.

Table 2. The effect of the support: reaction conditions, propylene selectivity, propylene yield and deactivation rate per selected catalyst of each article.

Catalyst	Reaction Conditions	Reactor	Time on Stream Test	Propylene Selectivity (S) and Yield (Y)	Deactivation Rate ^a	Ref.
Pt/Ga/Al ₂ O ₃	C ₃ H ₈ /N ₂ = 1:9 WHSV = 2.4 h ⁻¹	Fixed bed i.d. = 8 mm	100 kPa 853 K 2 h	S > 97% Y > 46%	0.373 h ⁻¹	[55]
Pt-Sn ₂ /meso-Al ₂ O ₃	C ₃ H ₈ /H ₂ /N ₂ = 1/1/3 WHSV = 2.9 h ⁻¹	Fixed bed -	853 K 160 h	S > 95% Y > 38%	0.0033 h ⁻¹	[56]
Pt-Sn/TiO ₂ Al ₂ O ₃	C ₃ H ₈ /H ₂ = 1/1 GHSV = 1600 h ⁻¹	Fixed bed -	1 atm 873 K 10 h	S > 88% Y > 23%	0.034 h ⁻¹	[59]
Pt _{0.5} -Ge _{1.5} /Al ₂ O ₃ - CaO	C ₃ H ₈ /H ₂ /N ₂ /Ar = 2/1/16.78/0.22 WHSV = 23.5 h ⁻¹	Fixed bed i.d. = 5 mm	1 atm 873 K 25 h	S > 98% Y > 16%	0.013 h ⁻¹	[60]
PtSnK/Al ₂ O ₃	H ₂ /C ₃ H ₈ = 1/2 WHSV = 4 h ⁻¹	Fixed bed i.d. = 10 mm l = 450 mm	1 atm 873 K 50 h	S = 96.5% Y = 32.8%	0.005 h ⁻¹	[61]
PtSn/beta (300)	N ₂ /C ₃ H ₈ = 1/10 WHSV = 6 h ⁻¹	Fixed bed -	1 atm 893 K 4 h	S = 65.5% Y = 21.6%	0.319 h ⁻¹	[62]
Pt/Sn (1.0)/Na-BEA-D	C ₃ H ₈ = 1 WHSV = 3.5 h ⁻¹	Fixed bed -	1 atm 823 K 4 h	S = 98.8% Y = 25.7%	0.025 h ⁻¹	[63]
Pt-SnO _x /10% TS-1@SBA-16	C ₃ H ₈ /H ₂ /N ₂ = 1/1/4 WHSV = 3 h ⁻¹	Fixed bed -	1 atm 863 K 7 h	S = 96.5% Y = 49.5%	0.018 h ⁻¹	[64]
PtSn/B-ZrO ₂	C ₃ H ₈ /H ₂ /N ₂ = 1/1/8 WHSV = 3 h ⁻¹	Fixed bed i.d. = 8 mm	1 atm 823 K 5 h	S > 99.5% Y > 34.3%	0.0127 h ⁻¹	[65]

Table 2. Cont.

Catalyst	Reaction Conditions	Reactor	Time on Stream Test	Propylene Selectivity (S) and Yield (Y)	Deactivation Rate ^a	Ref.
K-PtSn@MFI	C ₃ H ₈ /N ₂ = 5/16 WHSV = 1.85 h ⁻¹	Fixed bed -	1 atm 873 K 65 h	S = 97.5% Y = 46.3%	0.013 h ⁻¹	[67]
Zn(Ni)Ti(0.4%Pt)O ₃ /SiO ₂	C ₃ H ₈ /H ₂ /N ₂ = 8/7/35 WHSV = 3 h ⁻¹	Fixed bed -	1 atm 873 K 14 h	S = 96.6% Y = 26.6 %	0.061 h ⁻¹	[69]
0.3Pt/0.5Sn-Si-beta	C ₃ H ₈ /N ₂ = 1/19 WHSV = 1 h ⁻¹	Fixed bed i.d. = 5 mm	1 atm 823 K 24 h	S = 94% Y = 24.4%	0.002 h ⁻¹	[70]
Pt-Sn ₂ /SnBeta	C ₃ H ₈ /H ₂ /N ₂ = 1/1/8 WHSV = 140 h ⁻¹	Fixed bed i.d. = 6 mm	1 atm 843 K 159 h	S = 99% Y = 42%	0.0063 h ⁻¹	[71]
0.3Pt0.5Zn@S-1	C ₃ H ₈ /N ₂ = 11/19 WHSV = 6.5 h ⁻¹	Fixed bed i.d. = 5 mm	1 atm 823 K 60 h	S = 99.8% Y = 42.4%	0.002 h ⁻¹	[72]
PtZn ₄ @S-1-H	C ₃ H ₈ /N ₂ = 1/3 WHSV = 3.6 h ⁻¹	Fixed bed i.d. = 20 mm	1 atm 823 K 217 h	S = 99.2% Y = 40.1%	0.001 h ⁻¹	[73]
PtSn/Fe-S1	C ₃ H ₈ /Ar = 20/80 WHSV = 4.05 h ⁻¹	Fixed bed i.d. = 10 mm l = 200 mm	1 atm 853 K 50 h	S = 95% Y = 18.3%	0.03 h ⁻¹	[74]
GaPt@S-1	C ₃ H ₈ /N ₂ = 1/19 WHSV = 0.65 h ⁻¹	Fixed bed i.d. = 5 mm	1 atm 873 K 24 h	S = 95% Y = 39.4%	0.0068 h ⁻¹	[75]
PtGa@MFI	C ₃ H ₈ /H ₂ /N ₂ = 1/1/2. WHSV = 5.9 h ⁻¹	Fixed bed i.d. = 10 mm	1 atm 873 K 20 h	S = 98% Y = 14.3%	0.027 h ⁻¹	[76]

Table 2. Cont.

Catalyst	Reaction Conditions	Reactor	Time on Stream Test	Propylene Selectivity (S) and Yield (Y)	Deactivation Rate ^a	Ref.
0.7Pt0.7Zn/MZ	C ₃ H ₈ = 1 WHSV = 13 h ⁻¹	Fixed bed i.d. = 8 mm	853 K 600 h	S > 93% Y > 15%	0.0017 h ⁻¹	[77]
Pt/Si-MFI-NS	C ₃ H ₈ /N ₂ = 1/1 WHSV = 2.82 h ⁻¹	Fixed bed -	1 atm 823 K 13 h	S = 95% Y = 29.3%	0.022 h ⁻¹	[78]
PtSnNa/ZFS	H ₂ /C ₃ H ₈ = 1/4 WHSV = 3 h ⁻¹	Fixed bed -	0.1 MPa 863 K 100 h	S > 99.4% Y > 30.7%	0.004 h ⁻¹	[79]
Pt/P-CNTs	C ₃ H ₈ /N ₂ = 5/95 WHSV = 1.8 h ⁻¹	Fixed bed -	0.13 MPa 873 K 10 h	S > 85% Y > 4%	0.039 h ⁻¹	[80]
Pt-Sn/Al ₂ O ₃	C ₃ H ₈ /Ar = 1/2.8 WHSV = 36.5 h ⁻¹	Fixed bed i.d. = 4 mm	1 atm 873 K 36 h	S = 99.1% Y = 26.4%	0.017 h ⁻¹	[81]
Pt/Cu/h-BN-sheet	C ₃ H ₈ /H ₂ /N ₂ = 1/1/4	Fixed bed -	1 atm 793 K 6 h	S > 99.5% Y > 11.7%	0.05 h ⁻¹	[82]
PtIn/LaAlO/AIO	C ₃ H ₈ /H ₂ /N ₂ = 8/7/35 WHSV = 3 h ⁻¹	Fixed bed i.d. = 8 mm	1 atm 873 K 16 h	S > 90% Y > 25%	0.054 h ⁻¹	[83]
PtIn/HT	C ₃ H ₈ /H ₂ /N ₂ = 8/7/35 WHSV = 3 h ⁻¹	Fixed bed -	873 K 190 h	S > 95% Y > 34%	0.0035 h ⁻¹	[87]
Pt/MgAl(1.6In)O	C ₃ H ₈ = 1 WHSV = 1.6 h ⁻¹	Fixed bed i.d. = 19 mm	1 atm 873 K 5 h	S > 96% Y > 26%	0.013 h ⁻¹	[88]

Table 2. Cont.

Catalyst	Reaction Conditions	Reactor	Time on Stream Test	Propylene Selectivity (S) and Yield (Y)	Deactivation Rate ^a	Ref.
PtSn-Mg(3Zn)AlO	H ₂ /C ₃ H ₈ /N ₂ = 0.15/1/4 WHSV = 6.3 h ⁻¹	Fixed bed i.d. = 8 mm	1 atm 823 K 14 h	S > 99% Y > 40%	0.042 h ⁻¹	[89]
Au-Pt/MgAlO _x	H ₂ /C ₃ H ₈ = 0.25 WHSV = 8 h ⁻¹	Fixed bed -	1 atm 823 K 5 h	S > 99% Y > 9.7%	0.116 h ⁻¹	[90]

$$^a k_d = \frac{\ln\left(\frac{100-X_{end}}{X_{end}}\right) - \ln\left(\frac{100-X_{in}}{X_{in}}\right)}{t}; [40].$$

6. Reactor Configuration

The shape of the catalysts can play a decisive role in the catalytic activity, due to limitations to mass and heat transfer. Reaction kinetics and mathematical models of pellet catalysts, in a reactor, of $\text{WO}_3/\text{Si-Al}$ metathesis catalyst and $\text{PtIn}/\text{hydrotalcite}$ dehydrogenation catalyst were simulated using gPROMS [91]. Three types of pellet catalysts were compared, including dehydrogenation-core (MDM) and dehydrogenation-shell (DMD) and physically mixed pellet catalysts. The sensitivity analysis of the operating conditions, ratios, shapes and sizes of pellet catalysts showed that the DMD catalyst offered the highest catalytic performances including higher alkene yield and lower alkene loss factor.

Comparative studies between granular and monolithic catalysts ($\text{PtSnNa}/\text{ZSM-5}$) highlighted the better performance of the second type of reactor configuration [92]. The worst performance of the granular catalysts in the fixed-bed reactor was attributed to the disordered arrangement and to the resultant diffusion restriction. The granular catalysts reduced the contact time of propane with the active center and led to the deep dehydrogenation of propylene, reducing its selectivity. In the case of monolithic configuration, the propane concentration inside the channels was higher than that on the surface, thus facilitating the diffusion into the fluid. The regular straight channel improved the contact of propane and reduced the contact time of propylene, thus suppressing the deep dehydrogenation.

A possible strategy to improve the propylene selectivity and yield is the use of a membrane reactor. The reduction in the operating reaction temperature allows decreasing the extent of side reactions responsible for coke formation. The integration of the reaction unit with a Pd-based membrane for the recovery of hydrogen allows shifting the chemical equilibrium and obtaining high propane conversion even at a lower temperature than the conventional one. This kind of reactor configuration may lead to better stability of the catalyst and an increase in the operation time, avoiding catalyst regeneration [93]. Computational analysis demonstrated that higher propane conversion and hydrogen selectivity are obtained at high temperatures, sweep ratios and steam ratios; moreover, increasing the operating pressure enhances the hydrogen recovery, although it decreases the propane conversion, propylene selectivity and hydrogen selectivity [94].

A summary table (Table 3) is provided to summarize the best results in terms of propylene yield and selectivity and deactivation rate, from the article reviewed in this section.

Table 3. Reactor configuration: reaction conditions, propylene selectivity and deactivation rate per selected catalyst of each article.

Catalyst	Reaction Conditions	Reactor	Time on Stream Test	Propylene Selectivity (S) and Yield (Y)	Deactivation Rate ^a	Ref.
PtSnNa/ZSM-5	$\text{C}_3\text{H}_8/\text{H}_2 = 3/1$ WHSV = 155 h^{-1}	Fixed bed i.d. = 25 mm l = 650 mm	0.1 MPa 863 K 12 h	S > 95% Y > 23.5%	0.011 h^{-1}	[92]
PtSn-based catalyst Pd membrane	$\text{C}_3\text{H}_8/\text{H}_2\text{O} = 4/1$ WHSV = 8 h^{-1}	Fixed bed o.d. = 33.6 mm l = 400 mm w.t. = 3.78 mm	6 atm 773 K 40 h	S > 95% Y > 5%	0.005 h^{-1}	[93]
PtSn/ Al_2O_3 Pd-Ag membrane	$\text{C}_3\text{H}_8/\text{H}_2\text{O} = 4/1$ $\text{N}_2/\text{C}_3\text{H}_8 = 6$	Catalytic membrane reactor Membrane thickness = 0.006 mm Membrane length = 150 mm Number of tubes = 600	3 bar 823 K	S = 96.3% Y = 19%	-	[94]

$$^a k_d = \frac{\ln\left(\frac{100-X_{end}}{X_{end}}\right) - \ln\left(\frac{100-X_{in}}{X_{in}}\right)}{t}; [40].$$

7. Catalyst Regeneration and Coke Combustion Kinetics

An efficient regeneration is essential to carry out a PDH process, and a continuous process by the regenerator is essential to perform an efficient process. Regeneration is typically achieved by periodic coke burning to realize sustainable operation; thus, the coke combustion is a crucial aspect in the management of a propylene production plant by propane dehydrogenation.

The exact composition of the coke is, to date, the subject of study. It has been suggested that the coke formed on PtSn-based catalysts in PDH reaction mainly consists of three kinds of species: aliphatics, aromatics and pregraphite, with the aliphatic one constituting most of the deposit, with the C/H ratio of around 1.5 [95]. Raman studies on exhausted Pt-Sn/SBA-16 catalysts have shown an increase in coke crystal size from 60 to 180 min on stream and from 180 to 300 min under reaction [96]. These results are consistent with the so-called “coke migration phenomenon”, attributed to the coke movement near the particle to the support, or to the sintering of the metallic particle.

Thermal gravimetric analysis has been used to study the non-isothermal kinetics of coke combustion, generated from the PDH process in presence of Pt-Sn/Al₂O₃ catalysts [97]. Four different catalysts were prepared by varying the Pt/Sn ratio from 3/0.5 to 3/3 by weight, the catalytic activity was evaluated with a reactant mixture of C₃H₈ (30 mL/min) and H₂ (30 mL/min) at 893 K for 5 h and the kinetic parameters for coke combustion were calculated by evaluating the coke deposited through a thermogravimetric analyzer in the presence of air. Three nonisothermal models (Friedman, Flynn–Wall–Ozawa and Kissinger–Akahira–Sunose) were used to evaluate the activation energy and the best model to fit the experimental data. The Flynn–Wall–Ozawa model fit better in the case of 3Pt/Al₂O₃ and 3Pt-0.5Sn/Al₂O₃, while the three models equally fit the data of 3Pt-1Sn/Al₂O₃, 3Pt-2Sn/Al₂O₃ and 3Pt-3Sn/Al₂O₃. The activation energy increased with increasing Sn addition in the 3Pt/Al₂O₃ catalyst. Plotting the experimental data by using the Criado master-plot method, the second-order reaction was operative for $\alpha < 0.5$, and the first-order reaction for was operative for $\alpha > 0.5$ (α = degree of conversion). These results were attributed to the extent of pseudo-pyrolysis and oxidative combustion which may affect the TGA analysis.

The cofeeding of hydrogen decreases the coke formation rate and increases the stability of the catalyst by removing the precursor of coke, while the cofeeding of water decreases the coke formation while increasing the activity by decreasing the apparent activation energy of propane conversion [95].

Coke burning may result in extensive active metal sintering, so alternative regeneration processes have also been proposed, which make use of ozone, hydrogen and oxychlorination. Optimal conversion recovery has been obtained by treatment of Pt-Sn/Al₂O₃ catalysts, with 35% HCl, after coke burning [98]. HCl treatment seems to play a similar role as oxychlorination in redispersing the Pt particles and generating the Pt₃Sn alloy.

8. Conclusions and Future Perspective

The continuous growth in propylene demand as feedstock for a large variety of specialties has driven the research to design and optimize new production processes. Among them, PDH, which makes use of Pt-based catalytic systems, can be considered the most effective in providing high propylene selectivity and yield. Pt-based catalysts have been extensively studied both in theoretical and experimental studies. Promoted catalytic formulations, shapes and acid–base properties of the supports have been studied and optimized in order to suppress coke formation and particle sintering.

One of the strategies proposed, in the reviewed articles, to limit the sintering of active species lies in the use of supports that trap the nanoparticles. A widely used example of support of this type is zeolites. However, as reported in Section 3, recent studies have shown that in some cases, these structures can reduce the selectivity for propylene, as they delay the desorption of the propylene itself, increasing the likelihood of side reactions, for example leading to coke formation. This discrepancy suggests the need for further investigation. It would be desirable to have theoretical studies that compare trapping structures, with cavities of different shapes and sizes and perhaps different functionalities, to evaluate the morphological effect, to design trapping structures for active species but not for propylene.

The critical points of the PDH process are certainly the selectivity for propylene and the deactivation of the catalytic systems, which regulate the yield of the process. The need

for frequent regeneration steps reduces the productivity of the process and the life of the catalysts. The use of promoters such as Sn, trapping supports and the synergistic effect of geometric and electronic promotion, which prevent the aggregation of nanoparticulate metal species, appear to be effective strategies for obtaining efficient catalytic systems. The studies that we have proposed in this review article are extremely promising; selectivity of 99% has been reported, even for high temperatures that reach 873 K. Catalytic systems with yields that approach 50% after more than 60 h of reaction, such as K-PtSn@MFI, and yields of 30% after more than 700 h of reaction, as in the case of PtGa-CaPb/SiO₂, have been reported. Moreover, in both cases, regeneration of the catalysts with oxygen was achieved without evidence of deactivation. However, studies in real production conditions are lacking, in which catalytic systems are used for thousands of hours and regenerated dozens of times. It is not clear what would happen in these cases; this aspect should be deepened.

An aspect that has not yet been extensively studied for Pt-based catalysts is the reactor configuration; moreover, all the reviewed articles report studies carried out in laboratory-scale reactors. Studies on scale-up to pilot or industrial size are missing. The selectivity of these catalytic systems is strictly related to the increased reactivity of the reaction product with respect to the raw material; once formed, propylene is more reactive than propane, especially in cracking reactions, resulting in coke formation and thus limiting the stability of the catalysts. Therefore, since the propylene selectivity and yield of the overall PDH process are also affected by its reactivity, one way to improve the process performance may be the reduction in the persistence of propylene on the catalytic sites. One more strategy, which can be coupled to that just mentioned, is the minimization of the propylene conversion to coke in the homogeneous phase. In this sense, the design of reactors, by minimizing the residence time of propylene on the catalysts and in the hot zone of the reactor, could effectively prevent both the deactivation of the catalyst and the fouling of the reactor (due to the coke formation on the inner walls of the reactor), allowing the use of less sophisticated and more economical catalytic systems.

Author Contributions: M.M., E.M., G.F. and V.P. equally contributed to the conceptualization, methodology, software, validation, formal analysis, investigation, resources, data curation, writing—original draft preparation, writing—review and editing, visualization, supervision, project administration and funding acquisition of this manuscript. All authors have read and agreed to the published version of the manuscript.

Funding: This research has received funding from the European Union's Horizon 2020 Research and Innovation Programme under grant agreement No. 869896.

Acknowledgments: The authors wish to acknowledge Eng. Simona Renda for the valuable suggestions and support provided for the restart of the PDH plant.

Conflicts of Interest: The authors declare no conflict of interest.

References

1. Available online: <https://pubchem.ncbi.nlm.nih.gov/compound/propylene> (accessed on 15 June 2021).
2. Chen, S.; Pei, C.; Sun, G.; Zhao, Z.-J.; Gong, J. Nanostructured Catalysts toward Efficient Propane Dehydrogenation. *Acc. Mater. Res.* **2020**, *1*, 30–40. [[CrossRef](#)]
3. Hu, Z.-P.; Yang, D.; Wang, Z.; Yuan, Z.-Y. State-of-the-art catalysts for direct dehydrogenation of propane to propylene. *Chin. J. Catal.* **2019**, *40*, 1233–1254. [[CrossRef](#)]
4. Dai, Y.; Gao, X.; Wang, Q.; Wan, X.; Zhou, C.; Yang, Y. Recent progress in heterogeneous metal and metal oxide catalysts for direct dehydrogenation of ethane and propane. *Chem. Soc. Rev.* **2021**, *50*, 5590–5630. [[CrossRef](#)]
5. Available online: <https://www.sciencedirect.com/topics/engineering/shale-gas> (accessed on 16 June 2021).
6. Docherty, S.R.; Rochlitz, L.; Payard, P.-A.; Copéret, C. Heterogeneous alkane dehydrogenation catalysts investigated via a surface organometallic chemistry approach. *Chem. Soc. Rev.* **2021**, in press. [[CrossRef](#)] [[PubMed](#)]
7. Available online: <https://www.mcdermott.com/What-We-Do/Technology/Lummus/Petrochemicals/Olefins/Propylene-Production/Propane-Butane-Dehydrogenation> (accessed on 16 June 2021).
8. Available online: <https://www.hydrocarbonprocessing.com/news/2020/09/honeywell-uop-oleflex-technology-continues-growth-in-china> (accessed on 17 June 2021).

9. Li, C.; Wang, G. Dehydrogenation of light alkanes to mono-olefins. *Chem. Soc. Rev.* **2021**, *50*, 4359. [[CrossRef](#)]
10. Dong, S.; Altwater, N.R.; Mark, L.O.; Hermans, I. Assessment and comparison of ordered & non-ordered supported metal oxide catalysts for upgrading propane to propylene. *Appl. Catal. A-Gen.* **2021**, *617*, 118121. [[CrossRef](#)]
11. Perehodjuk, A.; Zhang, Y.; Kondratenko, V.A.; Rodemerck, U.; Linke, D.; Bartling, S.; Kreyenschulte, C.R.; Jiang, G.; Kondratenko, E.V. The effect of supported Rh, Ru, Pt or Ir nanoparticles on activity and selectivity of ZrO₂-based catalysts in non-oxidative dehydrogenation of propane. *Appl. Catal. A-Gen.* **2020**, *602*, 117731. [[CrossRef](#)]
12. Zhang, W.; Wang, H.; Jiang, J.; Sui, Z.; Zhu, Y.; Chen, D.; Zhou, X. Size Dependence of Pt Catalysts for Propane Dehydrogenation: From Atomically Dispersed to Nanoparticles. *ACS Catal.* **2020**, *10*, 12932–12942. [[CrossRef](#)]
13. Liu, Z.; Li, Z.; Li, G.; Wang, Z.; Lai, C.; Wang, X.; Pidko, E.A.; Xiao, C.; Wang, F.; Li, G.; et al. Single-Atom Pt⁺ Derived from the Laser Dissociation of a Platinum Cluster: Insights into Nonoxidative Alkane Conversion. *J. Phys. Chem. Lett.* **2020**, *11*, 5987–5991. [[CrossRef](#)]
14. Nakaya, Y.; Hirayama, J.; Yamazoe, S.; Shimizu, K.; Furukawa, S. Single-atom Pt in intermetallics as an ultrastable and selective catalyst for propane dehydrogenation. *Nat. Commun.* **2020**, *11*, 2838. [[CrossRef](#)]
15. Chen, J.Z.; Talpade, A.; Canning, G.A.; Probus, P.R.; Ribeiro, F.H.; Datye, A.K.; Miller, J.T. Strong metal-support interaction (SMSI) of Pt/CeO₂ and its effect on propane dehydrogenation. *Catal. Today* **2021**, *371*, 4–10. [[CrossRef](#)]
16. Zhang, H.; Wan, H.; Zhao, Y.; Wang, W. Effect of chlorine elimination from Pt-Sn catalyst on the behavior of hydrocarbon reconstruction in propane dehydrogenation. *Catal. Today* **2019**, *330*, 85–91. [[CrossRef](#)]
17. Xie, Z.; Li, Z.; Tang, P.; Song, Y.; Zhao, Z.; Kong, L.; Fan, X.; Xiao, X. The effect of oxygen vacancies on the coordinatively unsaturated Al-O acidbase pairs for propane dehydrogenation. *J. Catal.* **2021**, *397*, 172–182, in press. [[CrossRef](#)]
18. Deng, L.; Zhou, Z.; Shishido, T. Behavior of active species on Pt-Sn/SiO₂ catalyst during the dehydrogenation of propane and regeneration. *Appl. Catal. A-Gen.* **2020**, *606*, 117826. [[CrossRef](#)]
19. Wang, T.; Cui, X.; Winther, K.T.; Abild-Pedersen, F.; Bligaard, T.; Nørskov, J.K. Theory-Aided Discovery of Metallic Catalysts for Selective Propane Dehydrogenation to Propylene. *ACS Catal.* **2021**, *11*, 6290–6297. [[CrossRef](#)]
20. Sun, X.; Xue, J.; Ren, Y.; Li, X.; Zhou, L.; Li, B.; Zhao, Z. Catalytic Property and Stability of Subnanometer Pt Cluster on Carbon Nanotube in Direct Propane Dehydrogenation. *Chin. J. Chem.* **2021**, *39*, 661–665. [[CrossRef](#)]
21. Ye, C.; Peng, M.; Wang, Y.; Zhang, N.; Wang, D.; Jiao, M.; Miller, J.T. Surface Hexagonal Pt₁Sn₁ Intermetallic on Pt Nanoparticles for Selective Propane Dehydrogenation. *ACS Appl. Mater. Interfaces* **2020**, *12*, 25903–25909. [[CrossRef](#)]
22. Wang, J.; Chang, X.; Chen, S.; Sun, G.; Zhou, X.; Vovk, E.; Yang, Y.; Deng, W.; Zhao, Z.-J.; Mu, R.; et al. On the Role of Sn Segregation of Pt-Sn Catalysts for Propane Dehydrogenation. *ACS Catal.* **2021**, *11*, 4401–4410. [[CrossRef](#)]
23. Chen, S.; Zhao, Z.-J.; Mu, R.; Chang, X.; Luo, J.; Purdy, S.C.; Kropf, A.J.; Sun, G.; Pei, C.; Miller, J.T.; et al. Propane Dehydrogenation on Single-Site [PtZn₄] Intermetallic Catalysts. *Chem* **2021**, *7*, 387–405. [[CrossRef](#)]
24. Sun, X.; Liu, M.; Huang, Y.; Li, B.; Zhao, Z. Electronic interaction between single Pt atom and vacancies on boron nitride nanosheets and its influence on the catalytic performance in the direct dehydrogenation of propane. *Chin. J. Catal.* **2019**, *40*, 819–825. [[CrossRef](#)]
25. Aly, M.; Fornero, E.L.; Leon-Garzon, A.R.; Galvita, V.V.; Saeys, M. Effect of Boron Promotion on Coke Formation during Propane Dehydrogenation over Pt/γ-Al₂O₃ Catalysts. *ACS Catal.* **2020**, *10*, 5208–5216. [[CrossRef](#)]
26. Xiao, L.; Ma, F.; Zhu, Y.-A.; Sui, Z.-J.; Zhou, J.-H.; Zhou, X.-G.; Chen, D.; Yuan, W.-K. Improved selectivity and coke resistance of core-shell alloy catalysts for propane dehydrogenation from first principles and microkinetic analysis. *Chem. Eng. J.* **2019**, *377*, 120049. [[CrossRef](#)]
27. Purdy, S.C.; Ghanekar, P.; Mitchell, G.; Kropf, A.J.; Zemlyanov, D.Y.; Ren, Y.; Ribeiro, F.; Delgass, W.N.; Greeley, J.; Miller, J.T. Origin of Electronic Modification of Platinum in a Pt₃V Alloy and Its Consequences for Propane Dehydrogenation Catalysis. *ACS Appl. Energy Mater.* **2020**, *3*, 1410–1422. [[CrossRef](#)]
28. Jimenez-Izal, E.; Liu, J.-Y.; Alexandrova, A.N. Germanium as key dopant to boost the catalytic performance of small platinum clusters for alkane dehydrogenation. *J. Catal.* **2019**, *374*, 93–100. [[CrossRef](#)]
29. Zhang, Z.; Xu, W.; Ye, X.; Xi, Y.; Qiu, C.; Ding, L.; Liu, G.; Xiao, Q. Enormous passivation effects of a surrounding zeolitic framework on Pt clusters for the catalytic dehydrogenation of propane. *Catal. Sci. Technol.* **2021**, *11*, 5250–5259. [[CrossRef](#)]
30. Chang, Q.-Y.; Yin, Q.; Ma, F.; Zhu, Y.-A.; Sui, Z.-J.; Zhou, X.-G.; Chen, D.; Yuan, W.-K. Tuning Adsorption and Catalytic Properties of α-Cr₂O₃ and ZnO in Propane Dehydrogenation by Creating Oxygen Vacancy and Doping Single Pt Atom: A Comparative First-Principles Study. *Ind. Eng. Chem. Res.* **2019**, *58*, 10199–10209. [[CrossRef](#)]
31. Chang, Q.-Y.; Wang, K.-Q.; Hu, P.; Sui, Z.-J.; Zhou, X.-G.; Chen, D.; Yuan, W.-K.; Zhu, Y.-A. Dual-function catalysis in propane dehydrogenation over Pt₁-Ga₂O₃ catalyst: Insights from a microkinetic analysis. *AIChE J.* **2020**, *66*, 16232. [[CrossRef](#)]
32. Chang, Q.-Y.; Wang, K.-Q.; Sui, Z.-J.; Zhou, X.-G.; Chen, D.; Yuan, W.-K.; Zhu, Y.-A. Rational Design of Single-Atom-Doped Ga₂O₃ Catalysts for Propane Dehydrogenation: Breaking through Volcano Plot by Lewis Acid–Base Interactions. *ACS Catal.* **2021**, *11*, 5135–5147. [[CrossRef](#)]
33. Escorcía, N.J.; LiBretto, N.J.; Miller, J.T.; Li, C.W. Colloidal Synthesis of Well-Defined Bimetallic Nanoparticles for Nonoxidative Alkane Dehydrogenation. *ACS Catal.* **2020**, *10*, 9813–9823. [[CrossRef](#)]
34. Qiu, Y.; Li, X.; Zhang, Y.; Xie, C.; Zhou, S.; Wang, R.; Luo, S.-Z.; Jing, F.; Chu, W. Various Metals (Ce, In, La, and Fe) Promoted Pt/Sn-SBA-15 as Highly Stable Catalysts for Propane Dehydrogenation. *Ind. Eng. Chem. Res.* **2019**, *58*, 10804–10818. [[CrossRef](#)]

35. Wang, Z.; Chen, Y.; Mao, S.; Wu, K.; Zhang, K.; Li, Q.; Wang, Y. Chemical Insight into the Structure and Formation of Coke on PtSn Alloy during Propane Dehydrogenation. *Adv. Sustain. Syst.* **2020**, *4*, 2000092. [CrossRef]
36. Xu, Z.; Xu, R.; Yue, Y.; Yuan, P.; Bao, X.; Abou-Hamad, E.; Basset, J.-M.; Zhu, H. Bimetallic Pt-Sn nanocluster from the hydrogenolysis of a well-defined surface compound consisting of $[(\equiv\text{AlO})\text{Pt}(\text{COD})\text{Me}]$ and $[(\equiv\text{AlO})\text{SnPh}_3]$ fragments for propane dehydrogenation. *J. Catal.* **2019**, *374*, 391–400. [CrossRef]
37. Jung, J.-W.; Kim, W.-I.; Kim, J.-R.; Oh, K.; Koh, H.L. Effect of Direct Reduction Treatment on Pt-Sn/ Al_2O_3 Catalyst for Propane Dehydrogenation. *Catalysts* **2019**, *9*, 446. [CrossRef]
38. Motagamwala, A.H.; Almallahi, R.; Wortman, J.; Igenegbai, V.O.; Linic, S. Stable and selective catalysts for propane dehydrogenation operating at thermodynamic limit. *Science* **2021**, *373*, 217–222. [CrossRef]
39. Goncalves Cesar, L.; Yang, C.; Lu, Z.; Ren, Y.; Zhang, G.; Miller, J.T. Identification of a Pt₃Co Surface Intermetallic Alloy in Pt–Co Propane Dehydrogenation Catalysts. *ACS Catal.* **2019**, *9*, 5231–5244. [CrossRef]
40. Rimaz, S.; Luwei, C.; Kawi, S.; Borgna, A. Promoting effect of Ge on Pt-based catalysts for dehydrogenation of propane to propylene. *Appl. Catal. A-Gen.* **2019**, *588*, 117266. [CrossRef]
41. Fan, X.; Liu, D.; Sun, X.; Yu, X.; Li, D.; Yang, Y.; Liu, H.; Diao, J.; Xie, Z.; Kong, L.; et al. Mn-doping induced changes in Pt dispersion and Pt_xMn_y alloying extent on Pt/Mn-DMSN catalyst with enhanced propane dehydrogenation stability. *J. Catal.* **2020**, *389*, 450–460. [CrossRef]
42. Xie, L.; Chai, Y.; Sun, L.; Dai, W.; Wu, G.; Guan, N.; Li, L. Optimizing zeolite stabilized Pt-Zn catalysts for propane dehydrogenation. *J. Energy Chem.* **2021**, *57*, 92–98. [CrossRef]
43. Chen, C.; Sun, M.; Hu, Z.; Ren, J.; Zhang, S.; Yuan, Z.-Y. New insight into the enhanced catalytic performance of ZnPt/HZSM-5 catalysts for direct dehydrogenation of propane to propylene. *Catal. Sci. Technol.* **2019**, *9*, 1979. [CrossRef]
44. Zhu, X.; Wang, X.; Su, Y. Propane dehydrogenation over PtZn localized at Ti sites on TS-1 zeolite. *Catal. Sci. Technol.* **2021**, *11*, 4482. [CrossRef]
45. Ingale, P.; Knemeyer, K.; Preikschas, P.; Ye, M.; Geske, M.; d’Alnoncourt, R.N.; Thomas, A.; Rosowski, F. Design of PtZn nanoalloy catalysts for propane dehydrogenation through interface tailoring via atomic layer deposition. *Catal. Sci. Technol.* **2021**, *11*, 484. [CrossRef]
46. Taccardi, N.; Grabau, M.; Debuschewitz, J.; Distaso, M.; Brandl, M.; Hock, R.; Maier, F.; Papp, C.; Erhard, J.; Neiss, C.; et al. Gallium-rich Pd–Ga Phases as Supported Liquid Metal Catalysts. *Nat. Chem.* **2017**, *9*, 862–867. [CrossRef] [PubMed]
47. Bauer, T.; Maisel, S.; Blaumeiser, D.; Vecchietti, J.; Taccardi, N.; Wasserscheid, P.; Bonivardi, A.; Gorling, A.; Libuda, J. Operando DRIFTS and DFT Study of Propane Dehydrogenation over Solid- and Liquid-Supported GaxPty Catalysts. *ACS Catal.* **2019**, *9*, 2842–2853. [CrossRef] [PubMed]
48. Wolf, M.; Raman, N.; Taccardi, N.; Horn, R.; Haumann, M.; Wasserscheid, P. Capturing spatially resolved kinetic data and coking of Ga-Pt Supported Catalytically Active Liquid Metal Solutions during propane dehydrogenation in situ. *Faraday Discuss.* **2021**, *229*, 359–377. [CrossRef] [PubMed]
49. Sricharoen, C.; Jongsomjit, B.; Panpranot, J.; Praserttham, P. The key to catalytic stability on sol-gel derived SnO_x/SiO₂ catalyst and the comparative study of side reaction with K-PtSn/ Al_2O_3 toward propane dehydrogenation. *Catal. Today* **2021**, *375*, 343–351. [CrossRef]
50. Naseri, M.; Tahriri Zangeneh, F.; Taeb, A. The effect of Ce, Zn and Co on Pt-based catalysts in propane dehydrogenation. *React. Kinet. Mech. Catal.* **2019**, *126*, 477–495. [CrossRef]
51. Wang, G.; Lu, K.; Yin, C.; Meng, F.; Zhang, Q.; Yan, X.; Bing, L.; Wang, F.; Han, D. One-Step Fabrication of PtSn/ $\gamma\text{-Al}_2\text{O}_3$ Catalysts with La Post-Modification for Propane Dehydrogenation. *Catalysts* **2020**, *10*, 1042. [CrossRef]
52. Nakaya, Y.; Xing, F.; Ham, H.; Shimizu, K.; Furukawa, S. Doubly Decorated Platinum–Gallium Intermetallics as Stable Catalysts for Propane Dehydrogenation. *Angew. Chem. Int. Ed.* **2021**, in press. [CrossRef]
53. Chen, S.; Chang, X.; Sun, G.; Zhang, T.; Xu, Y.; Wang, Y.; Pei, C.; Gong, J. Propane dehydrogenation: Catalyst development, new chemistry, and emerging technologies. *Chem. Soc. Rev.* **2021**, *50*, 3315. [CrossRef]
54. Zhao, D.; Lund, H.; Rodemerck, U.; Linke, D.; Jiang, G.; Kondratenko, E.V. Revealing fundamentals affecting activity and product selectivity in non-oxidative propane dehydrogenation over bare Al_2O_3 . *Catal. Sci. Technol.* **2021**, *11*, 1386. [CrossRef]
55. Yu, Q.; Yu, T.; Chen, H.; Fang, G.; Pan, X.; Bao, X. The effect of Al^{3+} coordination structure on the propane dehydrogenation activity of Pt/Ga/ Al_2O_3 catalysts. *J. Energy Chem.* **2020**, *41*, 93–99. [CrossRef]
56. Zhu, X.; Wang, T.; Xu, Z.; Yue, Y.; Lin, M.; Zhu, H. Pt-Sn clusters anchored at $\text{Al}^{3+}_{\text{penta}}$ sites as a sinter-resistant and regenerable catalyst for propane dehydrogenation. *J. Energy Chem.* **2022**, *65*, 293–301. [CrossRef]
57. Jang, E.J.; Lee, J.; Jeong, H.Y.; Kwak, J.H. Controlling the acid-base properties of alumina for stable PtSn-based propane dehydrogenation catalysts. *Appl. Catal. A-Gen.* **2019**, *572*, 1–8. [CrossRef]
58. Guntida, A.; Wannakao, S.; Praserttham, P.; Panpranot, J. Acidic nanomaterials (TiO₂, ZrO₂, and Al_2O_3) are coke storage components that reduce the deactivation of the Pt-Sn/ $\gamma\text{-Al}_2\text{O}_3$ catalyst in propane dehydrogenation. *Catal. Sci. Technol.* **2020**, *10*, 5100. [CrossRef]
59. Wang, G.; Song, N.; Lu, K.; Zhang, Q.; Fu, H.; Bing, L.; Wang, F.; Wang, F.; Han, D. The tuning of TiO₂- Al_2O_3 composite support for the fabrication of PtSn-based catalysts with superior catalytic performance in the propane dehydrogenation. *Mater. Today Commun.* **2021**, *26*, 101753. [CrossRef]

60. Rimaz, S.; Chen, L.; Monzón, A.; Kawi, S.; Borgna, A. Enhanced selectivity and stability of Pt-Ge/Al₂O₃ catalysts by Ca promotion in propane dehydrogenation. *Chem. Eng. J.* **2021**, *405*, 126656. [[CrossRef](#)]
61. Shi, Y.; Li, X.; Rong, X.; Gu, B.; Wei, H.; Zhao, Y.; Wang, W.; Sun, C. Effect of Aging Temperature of Support on Catalytic Performance of PtSnK/Al₂O₃ Propane Dehydrogenation Catalyst. *Catal. Lett.* **2020**, *150*, 2283–2293. [[CrossRef](#)]
62. Lee, S.-U.; Lee, Y.-J.; Kwon, S.-J.; Kim, J.-R.; Jeong, S.-Y. Pt-Sn Supported on Beta Zeolite with Enhanced Activity and Stability for Propane Dehydrogenation. *Catalysts* **2021**, *11*, 25. [[CrossRef](#)]
63. Ivanushkin, G.G.; Smirnov, A.V.; Kots, P.A.; Ivanova, I.I. Modification of Acidic Properties of the Support for Pt-Sn/BEA Propane Dehydrogenation Catalysts. *Pet. Chem.* **2019**, *59*, 733–738. [[CrossRef](#)]
64. Hongda, L.; Zhen, Z.; Jiacheng, L.; Jianmei, L.; Linlin, Z.; Jiachen, S.; Xiaoqiang, F. Synthesis of Pt-SnOx/TS-1@SBA-16 Composites and Their High Catalytic Performance for Propane Dehydrogenation. *Chem. Res. Chin. Univ.* **2019**, *35*, 866–873. [[CrossRef](#)]
65. Ji, Z.; Miao, D.; Gao, L.; Pan, X.; Bao, X. Effect of pH on the catalytic performance of PtSn/B-ZrO₂ in propane dehydrogenation. *Chin. J. Catal.* **2020**, *41*, 719–729. [[CrossRef](#)]
66. Chen, J.Z.; Gao, J.; Probus, P.R.; Liu, W.; Wu, X.; Wegener, E.C.; Kropf, A.J.; Zemlyanov, D.; Zhang, G.; Yang, X.; et al. The effect of strong metal-support interaction (SMSI) on Pt-Ti/SiO₂ and Pt-Nb/SiO₂ catalysts for propane dehydrogenation. *Catal. Sci. Technol.* **2020**, *10*, 5973. [[CrossRef](#)]
67. Liu, L.; Lopez-Haro, M.; Lopes, C.W.; Li, C.; Concepcion, P.; Simonelli, L.; Calvino, J.J.; Corma, A. Regioselective generation and reactivity control of subnanometric platinum clusters in zeolites for high-temperature catalysis. *Nat. Mater.* **2019**, *18*, 866–873. [[CrossRef](#)]
68. Weckhuysen, B.M. Stable platinum in a zeolite channel. *Nat. Mater.* **2019**, *18*, 778–779. [[CrossRef](#)]
69. Liu, Y.; Li, Y.; Ge, M.; Chen, X.; Guo, M.; Zhang, L. Perovskite-Derived Pt-Ni/Zn(Ni)TiO₃/SiO₂ Catalyst for Propane Dehydrogenation to Propene. *Catal. Lett.* **2019**, *149*, 2552–2562. [[CrossRef](#)]
70. Wang, Y.; Hu, Z.-P.; Tian, W.; Gao, L.; Wang, Z.; Yuan, Z.-Y. Framework-confined Sn in Si-beta stabilizing ultra-small Pt nanoclusters as direct propane dehydrogenation catalysts with high selectivity and stability. *Catal. Sci. Technol.* **2019**, *9*, 6993. [[CrossRef](#)]
71. Xu, Z.; Yue, Y.; Bao, X.; Xie, Z.; Zhu, H. Propane Dehydrogenation over Pt Clusters Localized at the Sn Single-Site in Zeolite Framework. *ACS Catal.* **2020**, *10*, 818–828. [[CrossRef](#)]
72. Wang, Y.; Hu, Z.-P.; Lv, X.; Chen, L.; Yuan, Z.-Y. Ultrasmall PtZn bimetallic nanoclusters encapsulated in silicalite-1 zeolite with superior performance for propane dehydrogenation. *J. Catal.* **2020**, *385*, 61–69. [[CrossRef](#)]
73. Sun, Q.; Wang, N.; Fan, Q.; Zeng, L.; Mayoral, A.; Miao, S.; Yang, R.; Jiang, Z.; Zhou, W.; Zhang, J.; et al. Subnanometer bimetallic Platinum-Zinc cluster in Zeolites for propane dehydrogenation. *Angew. Chem. Int. Ed.* **2020**, *59*, 19450. [[CrossRef](#)] [[PubMed](#)]
74. Zhou, S.; Liu, S.; Jing, F.; Jiang, C.; Shen, J.; Pang, Y.; Luo, S.; Chu, W. Effects of Dopants in PtSn/M-Silicalite-1 on Structural Property and on Catalytic Propane Dehydrogenation Performance. *ChemistrySelect* **2020**, *5*, 4175–4185. [[CrossRef](#)]
75. Wang, Y.; Suo, Y.; Lv, X.; Wang, Z.; Yuan, Z.-Y. Enhanced performances of bimetallic Ga-Pt nanoclusters confined within silicalite-1 zeolite in propane dehydrogenation. *J. Colloid Interface Sci.* **2021**, *593*, 304–314. [[CrossRef](#)]
76. Zhang, B.; Zheng, L.; Zhai, Z.; Li, G.; Liu, G. Subsurface-Regulated PtGa Nanoparticles Confined in Silicalite-1 for Propane Dehydrogenation. *ACS Appl. Mater. Interfaces* **2021**, *13*, 16259–16266. [[CrossRef](#)]
77. Han, S.W.; Park, H.; Han, J.; Kim, J.-C.; Lee, J.; Jo, C.; Ryoo, R. PtZn Intermetallic Compound Nanoparticles in Mesoporous Zeolite Exhibiting High Catalyst Durability for Propane Dehydrogenation. *ACS Catal.* **2021**, *11*, 9233–9241. [[CrossRef](#)]
78. Wannapakdee, W.; Yutthalekha, T.; Dugkhuntod, P.; Rodponthukwaji, K.; Thivasasith, A.; Nokbin, S.; Witoon, T.; Pengpanich, S.; Wattanakit, C. Dehydrogenation of Propane to Propylene Using Promoter-Free Hierarchical Pt/Silicalite-1 Nanosheets. *Catalysts* **2019**, *9*, 174. [[CrossRef](#)]
79. Yongjuan, W.; Yuming, Z.; Shijian, Z.; Qiang, H.; Yangyang, Z. Effect of Morphological Structure of PtSnNa/ZSM-5 on Its Catalytic Performance in Propane Dehydrogenation. *China Pet. Process. Petrochem. Technol.* **2020**, *22*, 87–97. [[CrossRef](#)]
80. Jie, L.; Changcheng, L.; Zhijian, D.; Huidong, Z. Phosphorous-Modified Carbon Nanotube-Supported Pt Nanoparticles for Propane Dehydrogenation Reaction. *China Pet. Process. Petrochem. Technol.* **2019**, *21*, 7–14.
81. Gong, N.; Zhao, Z. Peony-like Pentahedral Al(III)-Enriched Alumina Nanosheets for the Dehydrogenation of Propane. *ACS Appl. Nano Mater.* **2019**, *2*, 5833–5840. [[CrossRef](#)]
82. Wang, L.; Wang, Y.; Zhang, C.-W.; Wen, J.; Weng, X.; Shi, L. A boron nitride nanosheet-supported Pt/Cu cluster as a high-efficiency catalyst for propane dehydrogenation. *Catal. Sci. Technol.* **2020**, *10*, 1248. [[CrossRef](#)]
83. Chen, X.; Ge, M.; Li, Y.; Liu, Y.; Wang, J.; Zhang, L. Fabrication of highly dispersed Pt-based catalysts on γ -Al₂O₃ supported perovskite Nano islands: High durability and tolerance to coke deposition in propane dehydrogenation. *Appl. Surf. Sci.* **2019**, *490*, 611–621. [[CrossRef](#)]
84. Belskaya, O.B.; Leont'eva, N.N.; Zaikovskii, V.I.; Kazakov, M.O.; Likholobov, V.A. Synthesis of layered magnesium-aluminum hydroxide on the γ -Al₂O₃ surface for modifying the properties of supported platinum catalysts. *Catal. Today* **2019**, *334*, 249–257. [[CrossRef](#)]
85. Kwon, D.; Kang, J.Y.; An, S.; Yang, I.; Jung, J.C. Tuning the base properties of Mg-Al hydrotalcite catalysts using their memory effect. *J. Energy Chem.* **2020**, *46*, 229–236. [[CrossRef](#)]

86. Belskaya, O.B.; Stepanova, L.N.; Nizovskii, A.I.; Kalinkin, A.V.; Erenburg, S.B.; Trubina, S.V.; Kvashnina, K.O.; Leont'eva, N.N.; Gulyaeva, T.I.; Trenikhin, M.V.; et al. The effect of tin on the formation and properties of Pt/MgAl(Sn)Ox catalysts for dehydrogenation of alkanes. *Catal. Today* **2019**, *329*, 187–196. [[CrossRef](#)]
87. Li, J.; Zhang, M.; Song, Z.; Liu, S.; Wang, J.; Zhang, L. Hierarchical PtIn/Mg(Al)O Derived from Reconstructed PtIn-hydrotalcite-like Compounds for Highly Efficient Propane Dehydrogenation. *Catalysts* **2019**, *9*, 767. [[CrossRef](#)]
88. Srisakwattana, T.; Watmanee, S.; Wannakao, S.; Saiyasombat, C.; Praserttham, P.; Panpranot, J. Comparative incorporation of Sn and In in Mg(Al)O for the enhanced stability of Pt/MgAl(X)O catalysts in propane dehydrogenation. *Appl. Catal. A-Gen.* **2021**, *615*, 118053. [[CrossRef](#)]
89. Wu, X.; Zhang, Q.; Chen, L.; Liu, Q.; Zhang, X.; Zhang, Q.; Ma, L.; Wang, C. Enhanced catalytic performance of PtSn catalysts for propane dehydrogenation by a Zn-modified Mg(Al)O support. *Fuel Process. Technol.* **2020**, *198*, 106222. [[CrossRef](#)]
90. Stepanova, L.N.; Belskaya, O.B.; Trenikhin, M.V.; Leont'eva, N.N.; Gulyaeva, T.I.; Likhobobov, V.A. Effect of Pt(Au)/MgAlOx catalysts composition on their properties in the propane dehydrogenation. *Catal. Today* **2021**, *378*, 96–105, in press. [[CrossRef](#)]
91. Sripinun, S.; Lorattanaprasert, K.; Gayapan, K.; Suriye, K.; Wannakao, S.; Praserttham, P.; Assabumrungrat, S. Design of hybrid pellet catalysts of WO₃/Si-Al and PtIn/hydrotalcite via dehydrogenation and metathesis reactions for production of olefins from propane. *Chem. Eng. Sci.* **2021**, *229*, 116025. [[CrossRef](#)]
92. Tong, Q.; Zhao, S.; Liu, Y.; Xu, B.; Yu, L.; Fan, Y. Design and synthesis of the honeycomb PtSnNa/ZSM-5 monolithic catalyst for propane dehydrogenation. *Appl. Organomet. Chem.* **2019**, *34*, 5380. [[CrossRef](#)]
93. Ricca, A.; Montella, F.; Iaquaniello, G.; Palo, E.; Salladini, A.; Palma, V. Membrane assisted propane dehydrogenation: Experimental investigation and mathematical modelling of catalytic reactions. *Catal. Today* **2019**, *331*, 43–52. [[CrossRef](#)]
94. Saidi, M.; Safaripour, M. Pure Hydrogen and Propylene Coproduction in Catalytic Membrane Reactor-Assisted Propane Dehydrogenation. *Chem. Eng. Technol.* **2020**, *43*, 1402–1415. [[CrossRef](#)]
95. Lian, Z.; Si, C.; Jan, F.; Zhi, S.K.; Li, B. Coke Deposition on Pt-Based Catalysts in Propane Direct Dehydrogenation: Kinetics, Suppression, and Elimination. *ACS Catal.* **2021**, *11*, 9279–9292. [[CrossRef](#)]
96. Ruelas-Leyva, J.P.; Maldonado-Garcia, L.F.; Talavera-Lopez, A.; Santos-López, I.A.; Picos-Corrales, L.A.; Santolalla-Vargas, C.E.; Torres, S.A.G.; Fuentes, G.A. A Comprehensive Study of Coke Deposits on a Pt-Sn/SBA-16 Catalyst during the Dehydrogenation of Propane. *Catalysts* **2021**, *11*, 128. [[CrossRef](#)]
97. Nasution, P.S.; Jung, J.-W.; Oh, K.; Koh, H.L. Coke combustion kinetics of spent Pt-Sn/Al₂O₃ catalysts in propane dehydrogenation. *Korean J. Chem. Eng.* **2020**, *37*, 1490–1497. [[CrossRef](#)]
98. Choi, Y.S.; Oh, K.; Jung, K.-D.; Kim, W.-I.; Koh, H.L. Regeneration of Pt-Sn/Al₂O₃ Catalyst for Hydrogen Production through Propane Dehydrogenation Using Hydrochloric Acid. *Catalysts* **2020**, *10*, 898. [[CrossRef](#)]